E-Article

A Trade-Off between Robustness to Environmental Fluctuations and Speed of Evolution

Max Schmid,[1,2] Maria Paniw,[1,3] Maarten Postuma,[1,4,5] Arpat Ozgul,[1] and Frédéric Guillaume[1,6,*]

1. Department of Evolutionary Biology and Environmental Studies, University of Zurich, Winterthurerstrasse 190, CH-8057 Zurich, Switzerland; 2. Department of Ecology and Evolution, University of Lausanne, Biophore, CH-1015 Lausanne, Switzerland; 3. Ecological and Forestry Applications Research Centre (CREAF), Campus de Bellaterra (UAB) Edifici C, ES-08193 Cerdanyola del Vallès, Spain; 4. Plant Ecology and Nature Conservation Group, Wageningen University, 6700 AA Wageningen, The Netherlands; 5. Department of Animal Ecology and Physiology, Radboud University, Nijmegen, The Netherlands; 6. Organismal and Evolutionary Biology Research Programme, University of Helsinki, Biocenter 3, 00014 Helsinki, Finland

Submitted June 9, 2021; Accepted January 6, 2022; Electronically published May 19, 2022

Online enhancements: supplemental PDF. *Dryad data:* https://doi.org/10.5061/dryad.hx3ffbgdv.

ABSTRACT: Understanding how a species' life history affects its capacity to cope with environmental changes is important in the context of rapid climate changes. Reinterpreting previous results from a well-developed theoretical framework, we show that a trade-off exists between a species' ability to genetically adapt to long-term gradual environmental changes and its ability to demographically resist short-term environmental perturbations, causing variation in its vital rates. Surprisingly, this important insight has not been made formally explicit before. Choosing archetypal life histories along the fast-slow pace-of-life continuum and modeling their eco-evolutionary dynamics, we further show that long-lived species have larger demographic robustness to interannual fluctuations but limited trait evolutionary responses in gradually changing environments. In contrast, short-lived species had larger evolvability but reduced demographic robustness. This trade-off bears heavily on extinction probabilities of populations tracking fast trait changes in stochastic environments. Faster trait evolution in short-lived species came at the expense of their higher sensitivity to short-term fluctuations, causing higher extinction rates than for long-lived species. Long-lived species persisted better on short timescales but built maladaptation and an extinction debt over time. This work shows how modeling species' eco-evolutionary dynamics can help to assess species vulnerability to environmental changes.

Keywords: environmental stochasticity, environmental change, life history strategies, evolvability, sensitivity, evolutionary rescue.

* Corresponding author; email: frederic.guillaume@helsinki.fi.

ORCIDs: Schmid, https://orcid.org/0000-0001-7197-4775; Paniw, https://orcid.org/0000-0002-1949-4448; Postuma, https://orcid.org/0000-0002-4317-2721; Ozgul, https://orcid.org/0000-0001-7477-2642; Guillaume, https://orcid.org/0000-0003-0874-0081.

Introduction

The environmental conditions to which a species adapts often fluctuate between years and can change gradually on decennial or centennial timescales. Adapting to both short-term and long-term environmental variations is a considerable challenge for species (Bürger and Lynch 1995; Boyce et al. 2006; Van De Pol et al. 2010; Vázquez et al. 2015). As an example of the two timescales of variation, average global temperatures have changed in the course of long-term glacial cycles or during recent rapid anthropogenic climate change, but they also vary between years, sometimes exhibiting extreme fluctuations (Stocker et al. 2013; Ummenhofer and Meehl 2017). Given that the environmental tolerance of all species is finite, the exposure to short- or long-term environmental changes can result in higher mortality, lower recruitment, and population declines. To persist in dynamic environments, species have to constantly adapt and adjust, and several ecological and evolutionary strategies exist to do so. Most often cited are changes in species' distributions when species are able to follow their ecological niche in space, plastic or evolutionary changes in phenology to follow their niche in time, or evolution of their niche via evolutionary adaptation to new conditions (Parmesan 2006; Aitken et al. 2008; Bell and Gonzalez 2009; Doak and Morris 2010; Duputié et al. 2015; Cayuela et al. 2017; McDonald et al. 2017). Yet we still have a poor understanding of how much species differ in either of these strategies and how such differences affect their ability to succeed and persist when facing environmental changes. Being able to categorize species relative to their capacity to withstand environmental fluctuations

  https://doi.org/10.1086/719654

and adapt to centennial trends in climatic changes will help us target conservation efforts and preserve biodiversity (e.g., Pearson et al. 2014). Doing so requires us to understand how species differences in their life history and evolutionary characteristics affect their capacity to persist demographically and adapt to new conditions genetically. It is known that life history characteristics affect both the robustness of a population against short-term environmental fluctuations (Caswell 2001; Boyce et al. 2006; Morris et al. 2008; Tuljapurkar et al. 2009) and the speed of adaptive evolution in response to gradual environmental change (Engen et al. 2011; Barfield et al. 2011; Orive et al. 2017). However, we miss an explicit treatment of the link between demographic robustness and the rate of evolutionary responses in fluctuating environments. In particular, we ask here how a life history's contribution to cope with short-term environmental variability might come at the cost of a poor evolutionary response to long-term changes and vice versa. To our knowledge, such a trade-off has not been made explicit in the literature to date.

Stochasticity in vital rates (survival and fecundity) from random environmental fluctuations reduces the long-run fitness of populations and may depress population sizes, thereby increasing extinction risks (Tuljapurkar 1982; Lande and Orzack 1988; Tuljapurkar et al. 2003; Engen et al. 2005; Sæther et al. 2013). How severely environmental variability feeds back on population growth can be described by the species' demographic robustness, which we define as being inversely proportional to the sensitivity of a species' growth rate to stochasticity in vital rates (see "Models"). A demographically robust species can cope well with stochastic environmental variation, as it experiences only little reduction in the growth rate or equilibrium population size from stochasticity in vital rates. The demographic robustness of a species depends on its life cycle, especially on its position along the fast-slow continuum and its reproductive strategy (Salguero-Gómez et al. 2017; Paniw et al. 2018). Theory shows that species with longer generation times (on the slow end of the continuum) are more robust to fluctuations than short-lived species (on the fast end of the continuum), as are more iteroparous compared with semelparous species (Murphy 1968; Tuljapurkar 1990; Tuljapurkar et al. 2009). Empirically, Morris et al. (2008) found a relation between the life expectancy of 36 plant and animal species and their sensitivity to environmentally driven variation in vital rates. Species with long generation times experienced less pronounced demographic consequences from stochasticity in vital rates than short-lived species (see also Dalgleish et al. 2010; Sæther et al. 2013). A species' sensitivity to environmental variability further depends on the proportion of individuals exposed to environmental variability. For instance, long-lived plants often exhibit highly tolerant age or stage classes, like seeds or adult trees, that can overcome detrimental conditions much better than seedlings or juveniles (Petit and Hampe 2006; Buoro and Carlson 2014) and help to "disperse through time" (Cohen 1967; Evans and Dennehy 2005; Buoro and Carlson 2014).

Life history strategies also shape the rate of trait evolution when the environment changes gradually (Lande 1982; Charlesworth 1994; Ellner and Hairston 1994; Engen et al. 2009, 2011; Barfield et al. 2011; Orive et al. 2017; Cotto et al. 2019). The generation time of a species, which affects the pace of life, is an indicator for how fast selection can translate into changes in the gene pool. The lower the generation time, the greater the evolutionary response to environmental change per unit of time is (Lande 1982; Vander Wal et al. 2013; Carlson et al. 2014; Orive et al. 2017). With life stages highly tolerant to environmental variation, life history strategies further control the proportion of individuals exposed to the environment. Those genotypes "hidden" in the seed bank or in highly tolerant adult stages are not under selection and thereby delay genetic changes at the population level (Templeton and Levin 1979; Hairston and De Stasio 1988; Barfield et al. 2011; Orive et al. 2017).

Together with the life history effects on robustness mentioned above, we can expect a trade-off between the rate of evolution and the demographic sensitivity to short-term environmental fluctuations. We can hypothesise that short-lived species will have faster evolutionary trait responses but suffer from a higher demographic sensitivity. In contrast, species with longer generation times should be demographically more robust but less evolutionarily responsive to changes in their environments. In fact, such a trade-off is implicit from previous theoretical work, even though it has not been explicitly described as such before. Lande (1982) and Barfield et al. (2011) described the evolutionary response to selection as a function of the growth rate sensitivity to vital rate changes, which is thus related to our definition of demographic robustness against short-term fluctuations (see also Tuljapurkar 1982, 1990). The trade-off was also suggested by the results of Templeton and Levin (1979) and Hairston and De Stasio (1988), who found that the presence of a seed bank slowed down the rate of phenotypic trait evolution. Still, the strongest support for the existence of the trade-off was provided by Orive et al. (2017), who found that elevated iteroparity slowed down evolution but increased survival after a step change in the environment. At this point, it is important to note that the expected trade-off between demographic robustness and evolvability is not a "classic" life history trade-off regarding individual decisions about resource allocation (e.g., Stearns 1989) but instead is a population property determined by life history.

While several findings point toward a robustness-evolvability trade-off among life history strategies, other studies hint at potential mechanisms to overcome this

trade-off. Species with overlapping generations were suggested to harbor higher levels of standing genetic variation in fluctuating environments than species with nonoverlapping generations, a process known as the genetic storage effect (Ellner and Hairston 1994; Sasaki and Ellner 1997; Svardal et al. 2015). Given that the rate of evolution increases with the amount of standing genetic variation, species with highly robust life stages and overlapping generations might be able to accumulate enough genetic variance and evolve faster, compensating for longer generation times (Yamamichi et al. 2019). All in all, this shows that life history strategies can have large effects on evolutionary and demographic dynamics and on the success of evolutionary rescue. Given that short- and long-term environmental changes often appear concurrently, it is important not only to study the response to each kind of environmental variation separately but also to understand the relationship between the rate of evolution and the demographic robustness of a population. The existence of a trade-off implies that some species would be prone to fast extinction in times of large environmental perturbations, while others may persist at the price of the build up of an extinction debt in future environmental conditions (Cotto et al. 2017). It is thus important to formally acknowledge the existence of such a trade-off and characterize its eco-evolutionary implications in the context of climate changes, as it is direly missing at the moment.

Our aim is to make explicit the existence of a trade-off between the rate of evolution and the demographic robustness of a population using the theoretical framework set by previous work in evolutionary quantitative genetics (Lande 1982; Barfield et al. 2011; Orive et al. 2017) and to test its importance by simulating eco-evolutionary dynamics in density-regulated populations exposed to fluctuating environments. To these ends, we first characterized the trade-off between demographic robustness and the rate of evolution of four life history strategies spanning the fast-slow continuum and different levels of iteroparity in stage-structured populations. To make fair comparisons, we use standardized life histories (see "Models") and account for processes that could overcome the trade-off. Our first analysis of the trade-off consists of numerical evaluations of the quantitative genetics formalism developed by Lande (1982) and Barfield et al. (2011), utilizing classical matrix population modeling (Caswell 2001). We highlight the existing linear trade-off between sensitivities of the equilibrium population size and growth rate and the rate of evolution of a quantitative trait. In a second step, we used individual-based simulations to model the eco-evolutionary dynamics of a single population for the same (standardized) life histories subject to both random interannual fluctuations and long-term gradual changes of the optimum trait value. The simulations further allowed us to account for demographic and genetic stochasticity and evolving additive genetic variance given that demographic and genetic processes (e.g., survival, reproduction, mutation, and recombination) were implemented as stochastic events. We could thus study the effect of the trade-off between robustness and evolvability on extinction risk from environmental changes.

Models

The Trade-Off

The trade-off between the rate of evolution and the demographic robustness to short-term environmental fluctuations is implied by previous theoretical results (Lande 1982; Barfield et al. 2011; Tuljapurkar 1982). The speed of evolution for quantitative traits in a stage-structured population was derived by Barfield et al. (2011) as

$$\Delta\bar{\mathbf{z}} = \frac{1}{\bar{\lambda}}\mathbf{G}\sum_{i,j}\frac{\partial\bar{\lambda}}{\partial\bar{a}_{ij}}\nabla_{\bar{z}j}\bar{a}_{ij}, \tag{1}$$

where $\partial\bar{\lambda}/\partial\bar{a}_{ij}$ is the sensitivity of the average growth rate $\bar{\lambda}$ to changes in the average vital rate $\bar{a}_{ij}$, $\bar{a}_{ij}$ is the vital rate of individuals in stage j contributing to stage i by transition or sexual reproduction (Caswell 2001), and $\nabla_{\bar{z}_j} = (\partial/\partial\bar{z}_1, \partial/\partial\bar{z}_2, \ldots, \partial/\partial\bar{z}_m)$ is the gradient operator with respect to trait means at stage j (Barfield et al. 2011). Equation (1) was obtained under the assumption of density-independent population dynamics leading to a stable stage distribution (SSD) and a transition matrix **A** that is nearly constant over time, weak selection, and the same mean phenotypes $\bar{\mathbf{z}}$ and genetic variance-covariance **G** for all stages j (see the discussion in Barfield et al. 2011, app. B).

Importantly, equation (1) shows that the rate of evolution depends linearly on the growth rate sensitivity to variation in vital rates $\partial\bar{\lambda}/\partial\bar{a}_{ij}$, which we will define as the inverse of the population's demographic robustness. This is justified because the sensitivity $\partial\bar{\lambda}/\partial\bar{a}_{ij}$ not only quantifies the decline in the population growth rate with a deterministic decrease in transition rate $\bar{a}_{ij}$ but also is an important determinant of the long-run growth rate with stochastic variation in vital rates (see Tuljapurkar 1982; Lande 2007). Tuljapurkar (1982) approximated the stochastic population growth rate $\log(\lambda_s)$ as

$$\log(\lambda_s) \approx \log(\lambda_0) - \frac{1}{2\lambda_0^2}\left(\frac{\partial\bar{\lambda}}{\partial\bar{a}_{ij}}\right)^2\sigma_{ij}^2, \tag{2}$$

with the geometric growth rate under stable conditions λ_0 and the variance in the vital rate σ_{ij} (Tuljapurkar 1982, p. 149). For a given degree of environmental stochasticity ($\sigma_{ij}^2 > 0$), the higher the growth rate sensitivity to the stochastic vital rate ($\partial\bar{\lambda}/\partial\bar{a}_{ij}$), the lower the long-term growth

rate of the species is (Tuljapurkar 1982). As a consequence, the demographic robustness of a species is inversely proportional to $\partial\bar{\lambda}/\partial\bar{a}_{ij}$, with a higher sensitivity indicating a lower demographic robustness. Equation (2) was derived for serially independent and small environmental fluctuations in a single transition rate, in the absence of density-dependent effects. While serial independence should be met when the average environment remains constant and environmental fluctuations are independently and identically distributed, this assumption should be broken in the course of directional environmental changes.

In the following, we present a more detailed evaluation of the expected trade-off using both numeric analysis and individual-based simulations when focusing on four specific life history strategies. While the following analysis is based four life histories with specific assumptions regarding stage structure and selection regime, equation (1) from Barfield et al. (2011) and equation (2) from Tuljapurkar (1982) still provide a general description of the trade-off between $\Delta\bar{\mathbf{z}}$ and $\partial\bar{\lambda}/\partial\bar{a}_{ij}$ beyond the explored examples.

Four Life History Strategies

We modeled a hermaphroditic species with three life stages (offspring [n_1], juveniles [n_2], and adults [n_3]) in a single random mating population. Environmental fluctuations affected only juvenile survival via stabilizing selection on a quantitative trait, while offspring and adult survival was constant over time. This corresponds to situations where the focal trait is expressed only at the juvenile stage (e.g., growth) and where offspring and adult individuals have much higher environmental tolerance (e.g., plant seeds or adult trees with high frost or drought tolerance) or dwell in much more stable habitats (e.g., Petit and Hampe 2006; Van De Pol et al. 2010; Marshall et al. 2016).

We focused on four distinct life history strategies along two axes—timing of maturation and degree of iteroparity—with two cases each: precocious (pre) and delayed (del) maturation as well as iteroparity (ite) and semelparity (sem). The life histories with combinations of delayed maturation and iteroparity (del-sem, del-ite, pre-ite) had three stages and overlapping generations (fig. 1*a*). The precocious, semelparous life cycle (pre-sem) had nonoverlapping generations modeled with only two stages, juveniles (offspring maturing immediately) and adults reproducing once and dying (fig. 1*b*). We modeled two growth scenarios, one of an exponentially growing population and one of a population that reached an equilibrium population density ($\hat{n}_T$) from intraspecific competition (fig. 1*c*, 1*d*).

In the absence of density regulation, offspring, juvenile, and adult individuals survived to the next year with average probability $\bar{\sigma}_1$, $\bar{\sigma}_2$, and $\bar{\sigma}_3$, respectively (fig. 1*a*, 1*b*). Offspring exclusively resulted from the sexual reproduction of hermaphroditic adults with an average per capita fecundity of $\bar{\phi}$. Offspring matured to juveniles with mean maturation probability $\bar{\gamma}$ and stayed in the offspring stage with probability $1 - \bar{\gamma}$ (e.g., staying in a seed bank).

With density regulation, average survival of juveniles was reduced by intraspecific competition $\bar{c}$ following the Ricker function ($\bar{c} = \exp(-bn_3)$) and thus declined with increasing adult number n_3 for overlapping generations and with juvenile number n_2 for nonoverlapping generations (to avoid competition across generations), depending on the competition coefficient b. We also modeled a Beverton-Holt density regulation and present the results in the supplemental PDF. In the absence of density regulation, competition survival was constant and set to $\bar{c} = 1$.

The demographic dynamics of the three-stage life cycles with delayed offspring maturation and iteroparous adults (del-sem, del-ite, and pre-ite) were modeled by the following matrix population model (MPM):

$$A_3 = \begin{pmatrix} \bar{\sigma}_1(1-\bar{\gamma}) & 0 & \bar{\phi} \\ \bar{\sigma}_1\bar{\gamma} & 0 & 0 \\ 0 & \bar{\sigma}_2\bar{c} & \bar{\sigma}_3 \end{pmatrix}. \tag{3}$$

The two-stage life cycle with precocious maturation and semelparous adults (pre-sem) was represented by the following MPM:

$$A_2 = \begin{pmatrix} 0 & \bar{\phi} \\ \bar{\sigma}_2\bar{c} & 0 \end{pmatrix}. \tag{4}$$

We standardized life histories for uniform maximum population sizes $\hat{n}_{\mathrm{Tmax}}$ in the absence of environmental variation and for uniform maximum population growth rates ($\bar{\lambda}_{\max}$ the intrinsic population growth rate in the absence of density regulation when $\bar{c} = 1$). Standardization to equal $\hat{n}_{\mathrm{Tmax}}$ was necessary because $\partial\hat{n}_T/\partial\bar{\sigma}_2$ is a function of $\hat{n}_{\mathrm{Tmax}}$, and $\hat{n}_{\mathrm{Tmax}}$ determines how quickly populations will reach critically low densities when exposed to detrimental environmental change (e.g., Gomulkiewicz and Holt 1995; Carlson et al. 2014). Standardization to equal $\bar{\lambda}_{\max}$ allowed us to compare populations with similar growth under nonequilibrium conditions. With this standardization we could compare our four life histories while keeping key demographic properties constant (fig. S1). We adjusted the fecundity $\bar{\phi}$ to reach equal $\bar{\lambda}_{\max}$ across life histories and a standardized form of the competition coefficient b to reach equal $\hat{n}_{\mathrm{Tmax}}$ (see apps. A, B).

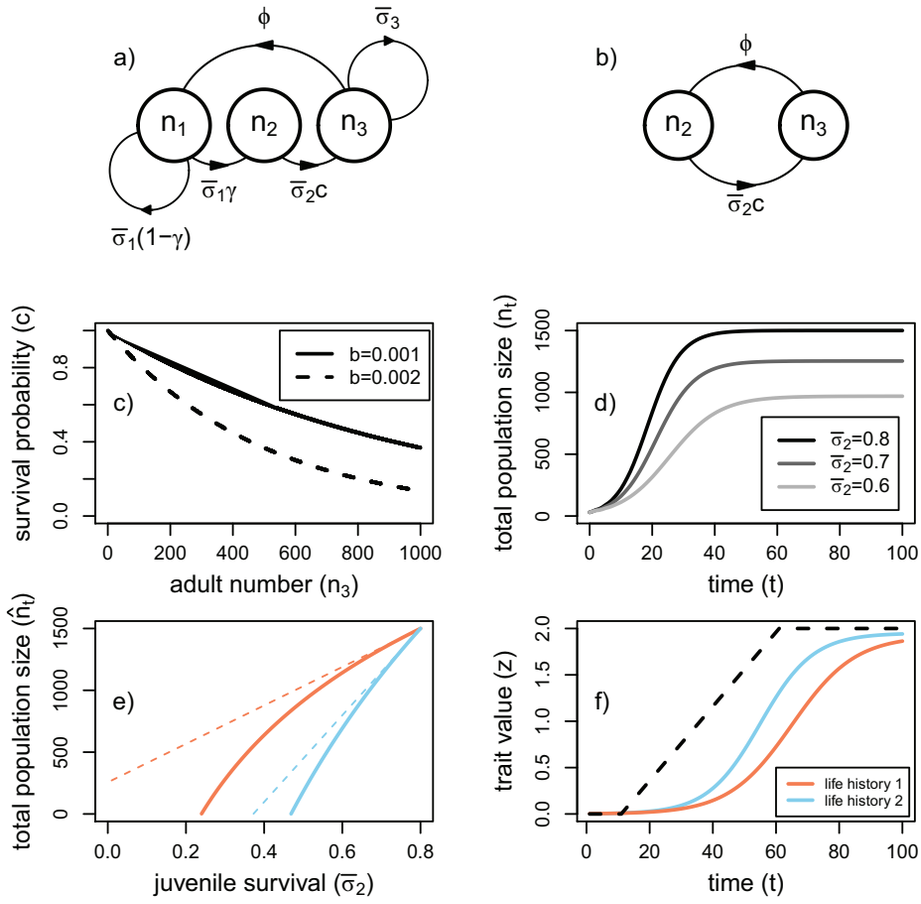

Figure 1: The life history plot in panel *a* illustrates the three-stage life cycle with delayed maturation and/or iteroparous adults (del-sem, del-ite, pre-ite), while the one in panel *b* shows the biennial two-stage life cycle (pre-sem, with precocious maturation and semelparous adults), together with the relevant vital rates. The graph in panel *c* demonstrates the effect of negative density dependence in the three-stage life cycle when juvenile survival is reduced by a factor *c* with increasing adult number (n_3), based on the Ricker function with competition coefficient $b = 0.001$ (solid line) and $b = 0.002$ (dashed line). The graph in panel *d* illustrates the temporal change in total population size over time following logistic growth such that an equilibrium mean population size is achieved from negative density dependence. By reducing the average juvenile survival $\bar{\sigma}_2$—for instance, from environmental perturbations—the population size at equilibrium $\hat{n}_T$ is reduced. We used the sensitivity of the equilibrium population size to juvenile survival ($\partial\hat{n}_T/\partial\bar{\sigma}_2$) as a measure for demographic robustness. In the graph in panel *e*, two life histories are shown with the same equilibrium population size ($\hat{n}_T$; the two solid lines) when environmental fluctuations are absent (at $\bar{\sigma}_2 = 0.8$) but with different sensitivities to reductions in juvenile survival from interannual fluctuations. The slope of the tangents at $\bar{\sigma}_2 = 0.8$ (dashed lines) in panel *e* represents $\partial\hat{n}_T/\partial\bar{\sigma}_2$ as how quickly $\hat{n}_T$ responds to small reductions in $\bar{\sigma}_2$. The graph in panel *f* illustrates the scenario with directional environmental change and the corresponding trait evolution of two life histories (the two solid lines). Environmental change is realized via directional changes of the phenotypic optima (θ, dashed line).

Numerical Evaluations

The Rate of Trait Evolution. We quantified the speed of evolution of a life history as the average asymptotic trait change $\Delta\bar{z}$ per time step t from genetic evolution (not plasticity) in response to directional selection. We will thus use $\Delta\bar{z}$ as a measure of evolvability e, as defined by Hansen et al. (2019): $e = \Delta\bar{z}/\beta(\bar{z}) = G$, or $e = \Delta\bar{z}$ for a standardized selection gradient $\beta(\bar{z}) = 1$ (the partial regression coefficient of relative fitness on the trait). Evolvability here broadly refers to the "ability to evolve" (e.g., Hansen and Houle 2008) and might vary with life history strategies even when the additive genetic variance G and the selection gradient $\beta(\bar{z})$ take uniform values. With only a subset of the population exposed to selection, only a part of the additive genetic variance contributes to annual trait changes. The results of Barfield et al. (2011) thus provide the possibility of applying the evolvability concept more precisely to stage-structured life histories, which has not been done to date.

For a species with three life history stages with one trait under selection in juveniles (z_2), the asymptotic rate

of evolution can be derived from equation (8) in Barfield et al. (2011), as detailed in appendix A:

$$\Delta\bar{z}_{\text{exp}} = \frac{1}{\bar{\lambda}} v_3 w_2 \bar{\sigma}_2 G_2 \beta(\bar{z}_2). \quad (5)$$

The asymptotic rate of trait change $\Delta\bar{z}$ thus varies with the additive genetic variance in juveniles (G_2), the selection gradient on a single juvenile trait ($\beta(\bar{z}_2)$), the fraction of individuals exposed to selection (w_2, the proportion of juveniles at SSD), the survival probability of these individuals ($\bar{\sigma}_2 = \sigma_{2\,\max}\bar{W}(\bar{z})$), and their contribution to the subsequent generations (v_3, the reproductive value of adults standardized such that $v^{\mathrm{T}}w = 1$; Barfield et al. 2011, eq. [8]). The rate of evolution ($\Delta\bar{z}_{\text{exp}}$) can thus be expressed as a function of the vital rates by deriving expressions for w_2 and v_3 (see app. A; see app. B for the two-stage life cycle). We assume here that variation in survival is caused by the phenotypic mismatch of the population with its environment, which affects only the vital rate of juveniles $\bar{a}_{32}$. The relationship between mean phenotypic trait value $\bar{z}$ and $\bar{a}_{32}$ is given by $\bar{a}_{32} = \sigma_{2\,\max}\bar{c}\,\bar{W}(\bar{z})$, the product of maximum juvenile survival ($\sigma_{2\max}$), competition survival ($\bar{c}$), and average juvenile survival depending on the mismatch between the population mean phenotype and the environment ($\bar{W}(\bar{z})$).

Beside the derivations for exponentially growing populations, we also derived the expected evolutionary responses to selection for populations at equilibrium population density ($\Delta\bar{z}_{\text{dd}}$; see apps. A, B). With density-dependent population growth, we assume that the rate of evolution can be approximated from the Lande theorem as well (Barfield et al. 2011, eq. [8]), at least in the absence of density-dependent selection when the population reached equilibrium density ($\bar{\lambda} = 1$) and when population dynamics are faster than evolutionary dynamics. Then, competition survival $\bar{c}$ and the transition matrix $\mathbf{A}$ are nearly constant over time, and the population reached SSD while not being at the phenotypic optimum yet.

Population Sensitivity to Environmental Fluctuations. For our exponentially growing populations with only juvenile survival changing with the environment, the growth rate sensitivity as a measure for demographic robustness becomes $\partial\bar{\lambda}/\partial\bar{\sigma}_2$. We computed $\partial\bar{\lambda}/\partial\bar{\sigma}_2$ for each life history variant using explicit derivations obtained with Mathematica 12.1 (Wolfram Research 2020). With density regulation, an alternative measure for demographic robustness is the sensitivity of the total population size at equilibrium $\hat{n}_{\mathrm{T}}$ to juvenile survival ($\partial\hat{n}_{\mathrm{T}}/\partial\bar{\sigma}_2$; see also fig. 1*e*). The sensitivity $\partial\hat{n}_{\mathrm{T}}/\partial\bar{\sigma}_2$ determines by how much a reduction in juvenile survival from environmental perturbation depresses total population density. As $\partial\hat{n}_{\mathrm{T}}/\partial\bar{\sigma}_2$ is often but not necessarily proportional to $\partial\bar{\lambda}/\partial\bar{\sigma}_2$ (as repeatedly described in Takada and Nakajima 1998; Grant and Benton 2000, 2003; Caswell et al. 2004), we present the results for both sensitivity measures in parallel. We derived the partial derivative of $\hat{n}_{\mathrm{T}}$ with respect to $\bar{\sigma}_2$ depending on single vital rates, as detailed in appendixes A and B.

Using the derivations from appendixes A and B, we explored the effect of the vital rates $\bar{\sigma}_1$, $\bar{\sigma}_3$, and $\bar{\gamma}$ on the trade-off between demographic robustness ($\partial\hat{n}_{\mathrm{T}}/\partial\bar{\sigma}_2$, $\partial\bar{\lambda}_{\mathrm{T}}/\partial\bar{\sigma}_2$) and evolvability ($\Delta\bar{z}$, with uniform $G = \beta(\bar{z}_2) = 1$ among life histories).

Individual-Based Simulations

We ran individual-based simulations to test our mathematical derivations and account for genetic and demographic stochasticity and an evolving additive genetic variance that varied between life histories. Simulations were run with Nemo (Guillaume and Rougemont 2006) extended for stage-structured populations (Cotto et al. 2017, 2020). We simulated a single panmictic population of hermaphroditic individuals. The population reached an equilibrium population size by density-dependent juvenile survival. A single quantitative trait was under hard selection in the juvenile stage. The following life cycle events occurred consecutively each year: density-dependent regulation (of juvenile survival from intraspecific competition using the Ricker function), viability selection (removal of juveniles according to their survival probability, which varied with the distance between trait value and environment), sexual reproduction (independent from the environmental state or population density), and stage transitions according to the MPM.

We modeled the four generic life history strategies presented in the previous section. We standardized all four life history strategies for the same total population size in the absence of environmental fluctuations ($\hat{n}_{\mathrm{Tmax}} = 1{,}500$ by adjusting b) and the same maximum population growth rate ($\bar{\lambda}_{\max} = 1.10$ or $\bar{\lambda}_{\max} = 1.15$ by adjusting ϕ). The single vital rates are listed in table S1. With these simulation scenarios we tried to span a range of key life history characteristics by accounting for differences in "pace of life" along the slow-fast continuum and for differences in the reproductive strategy (see fig. S2; Stearns 1983; Gaillard et al. 1989, 2005; Salguero-Gómez 2017).

Genetic Setup and Selection Model. We simulated the evolutionary dynamics of adaptation to a single environmental condition via the evolution of a single quantitative trait (z) under stabilizing selection in the juvenile stage using the classical Gaussian survival function $W(z) = \exp(-(z-\theta)^2/(2\omega^2))$, with θ the trait phenotypic optimum and ω^2 the width of the survival function. We set $\omega^2 = 4$ (corresponding to stronger selection) or $\omega^2 = 16$

(representing weaker selection). Each individual carried $l = 20$ unlinked loci, contributing additively to the trait z. We used a continuum-of-allele model where mutational effects, picked from a Gaussian distribution centered on zero with mutational variance $\alpha = 0.1$, were added to the existing allelic values. The mutation rate was $\mu = 0.0001$ so that the mutational phenotypic variance was $V_M = 2l\mu\alpha = 0.001$. We excluded random environmental effects on phenotype expression (e.g., developmental noise) for simplicity.

Environmental Scenarios. We simulated environmental variation between years together with gradual changes in the average condition by perturbing the phenotypic optimum θ (e.g., see Chevin et al. 2017). Each year, the position of the phenotypic optimum for the entire population was picked from a Gaussian distribution $\theta \sim \mathcal{N}(\bar{\theta}, \epsilon)$ with the average environment $\bar{\theta}$ and variance ϵ. We thus simulated environmental fluctuations between years that were independently and identically distributed (e.g., see Caswell 2001).

To allow the population genetic variance to reach mutation-selection-drift balance, we ran burn-in simulations for 50,000 years for each life history. Burn-in simulations were run with a constant average environment of $\bar{\theta} = 10$ for six different degrees of environmental fluctuations (with variance $\epsilon = 0.0$, 0.2, 0.5, 1.0, 1.5, and 2.0).

To assess the population size sensitivity of life history strategies to interannual environmental stochasticity, we recorded population demographic characteristics (e.g., population size $\hat{n}_T$) every 10 years for an additional period of 500 years. A life history's population size sensitivity was assessed as the steepness of declining average population sizes ($\hat{n}_T = (1/51)\sum_{t=1}^{51} n_T$) with increasing degrees of interannual environmental fluctuations ϵ. To assess the speed of trait evolution, we then initiated directional environmental change of the average environmental condition ($\bar{\theta}$) after burn-in while still simulating interannual variation on top of the changing mean. The average phenotypic optimum started to change at $t = 100$ with a rate of $\Delta\bar{\theta} = +0.01$, for 200 and 800 years. We quantified the speed of evolution as the time to reach 90% of the novel phenotypic optimum ($\bar{\theta} = 12$ or $\bar{\theta} = 18$). We did not use the maximum rate of phenotypic change per time step because all populations either became extinct or adopted trait changes as fast as the rate of environmental change ($\Delta\bar{z} = \Delta\bar{\theta}$).

Results

Mathematical Models

As expected from equation (1), we found a positive linear trade-off in the relationship between the rate of evolution ($\Delta\bar{z}$) and the sensitivity of the population size to juvenile survival ($\partial\hat{n}_T/\partial\bar{\sigma}_2$ and $\partial\bar{\lambda}/\partial\bar{\sigma}_2$) for both the three-stage model and the two-stage model (figs. 2, S3, S4). When comparing life histories with the same maximum growth rate, changes in vital rates that enhanced the rate of evolution also increased the sensitivity to environmental perturbations and vice versa.

A higher degree of iteroparity (high adult survival $\bar{\sigma}_3$; fig. 3*a*, 3*d*, 3*g*) and delayed maturation (low maturation rate $\bar{\gamma}$; fig. 3*c*, 3*f*, 3*i*) increased the robustness of the population size to environmental fluctuations (lower sensitivity $\partial\hat{n}_T/\partial\bar{\sigma}_2$) but reduced the rate of trait evolution (smaller $\Delta\bar{z}_{dd}$). In contrast, life histories with precocious maturation and semelparous adults allowed for fast evolution but had a reduced robustness to environmental variability. We obtained qualitatively similar results for the sensitivity of the growth rate $\partial\bar{\lambda}/\partial\bar{\sigma}_2$, at least for a given maximal growth rate (fig. 3*g*, 3*h*, 3*i*). In our models, iteroparity in adults and delayed maturation of offspring were associated with larger generation times and resulted in a smaller proportion of juveniles exposed to selection and lower contributions of these juveniles to future generations (fig. 2*c*, 2*d*; table S1).

The maximum rate of population growth ($\bar{\lambda}_{max}$) shaped both the population size and the growth rate sensitivity to environmental fluctuations (fig. 2*a*, 2*b*), even though it had no effect on the rate of evolution at carrying capacity ($\Delta\bar{z}_{dd}$; fig. 2*a*, 2*b*) and only minor effects on evolvability with exponential growth ($\Delta\bar{z}_{exp}$; see table S1). Higher $\bar{\lambda}_{max}$, when realized by higher fecundity, reduced $\partial\hat{n}_T/\partial\bar{\sigma}_2$ and thus helped to maintain higher population densities with short-term environmental perturbations (figs. 2*b*, 3*b*). However, higher $\bar{\lambda}_{max}$ increased $\partial\bar{\lambda}/\partial\bar{\sigma}_2$ (figs. 2*a*, 3*h*). With a greater maximum growth rate, juveniles contributed more to the next generation (resulting from a higher reproductive value after transition to the adult stage; table S1) such that changes in $\bar{\sigma}_2$ translated into greater changes in λ. In contrast, the equilibrium population density was less sensitive to juvenile survival, as a higher fecundity helped the population to recover more quickly from detrimental environmental events.

Results for a Beverton-Holt instead of a Ricker function for density regulation were qualitatively similar. The linear robustness-evolvability trade-off remained (fig. S5). Only the population size sensitivity $\partial\bar{\lambda}_T/\partial\bar{\sigma}_2$ was higher with a Beverton-Holt regulation function (fig. S6). The trade-off between evolvability and demographic robustness was also found for exponentially growing populations, with a positive linear relationship between $\Delta\bar{z}_{exp}$ and $\partial\bar{\lambda}/\partial\bar{\sigma}_2$ (fig. S3) that translated into a negative relationship between $\Delta\bar{z}_{exp}$ and the stochastic growth rate log (λ_s) (fig. S4). Exponentially growing populations (with $\lambda > 1$) had a higher evolvability and a higher demographic

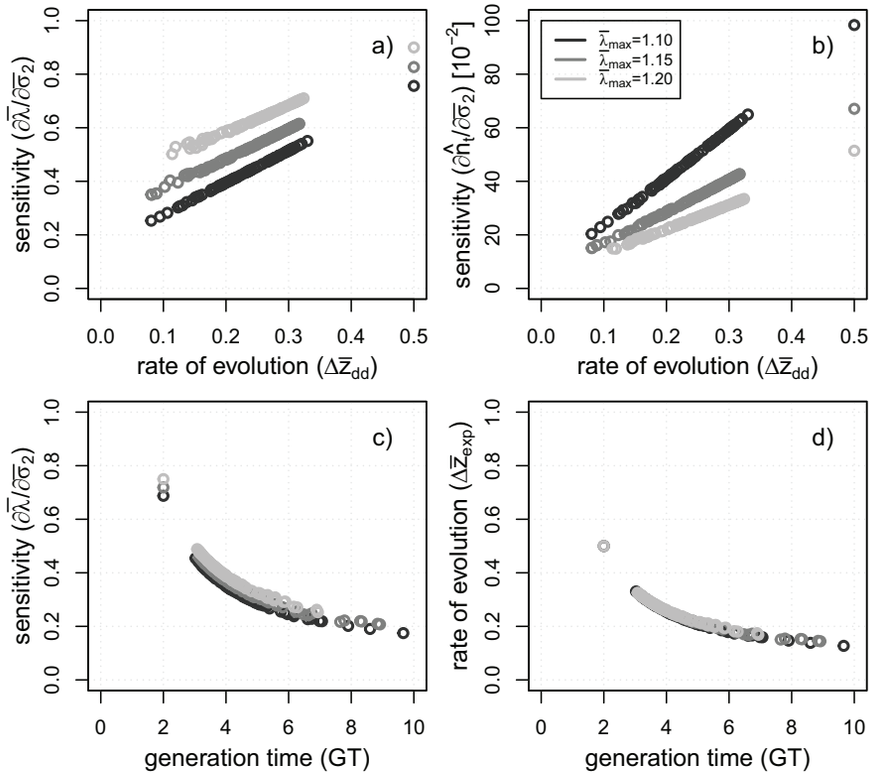

Figure 2: A life history's trade-off between evolvability ($\Delta\bar{z}_{dd}$) and robustness ($\partial\bar{\lambda}/\partial\bar{\sigma}_2$, $\partial\hat{n}_T/\partial\bar{\sigma}_2$) with density regulation at $\bar{\lambda} = 1$ are illustrated in panels *a* and *b*. Here, $\partial\hat{n}_T/\partial\bar{\sigma}_2$ was divided by 100 for better readability of the axis labels. In addition, the relation among robustness, evolvability, and generation time (all evaluated at exponential growth) are shown in panels *c* and *d*. Each circle illustrates a random combination of vital rates (with $0.2 \le \bar{\sigma}_1 \le 1.0$, $\bar{\sigma}_2 = 0.8$, $0.0 \le \bar{\sigma}_3 \le 0.9$, $0.2 \le \bar{\gamma} \le 1.0$). Fecundity ($\bar{\phi}$) was recalculated for each vital rate combination to standardize the maximum population growth rate ($\bar{\lambda}_{max} = 1.10$ − black, $\bar{\lambda}_{max} = 1.15$ − dark gray, $\bar{\lambda}_{max} = 1.20$ − light gray). For panels *a* and *b* the strength of competition (b) was recalculated for each life history variant to standardize for the same total population size ($\hat{n}_{Tmax} = 1{,}500$), respectively. We then computed the rate of evolution ($\Delta\bar{z}_{dd}$, with $G_2\beta(\bar{z}_2) = 1$, using eqq. [A23] and [B22]), the population size sensitivity ($\partial\hat{n}_T/\partial\bar{\sigma}_2$, using eqq. [A11] and [B11]), and the growth rate sensitivity ($\partial\bar{\lambda}/\partial\bar{\sigma}_2$, using explicit derivations from Mathematica). Generation time was computed with the popbio package (ver. 2.7; Stubben and Milligan 2007) in R (ver. 3.6.2; R Core Team 2019), which uses the method of section 5.3.5 in Caswell (2001). The three single points on the right of panels *a* and *b* were derived for the two-stage life cycle (with $\bar{\sigma}_2 = 0.8$), while the rest of the points illustrate parameter combinations for three-stage life cycles.

robustness (i.e., lower growth rate sensitivity) compared with the same populations at carrying capacity ($\lambda = 1$; fig. S7), a result of both higher juvenile survival and a larger growth rate in the absence of density regulation.

Individual-Based Simulations

We could also confirm the trade-off between evolvability and robustness in our individual-based simulations, as the life history effect on standing genetic variation (the genetic storage effect) was not strong enough to overcome the trade-off (figs. 4*c*, 5*d*). Species with high robustness had the slowest rates of evolution and vice versa. The average population size maintained at constant average conditions during burn-in declined with increasing environmental fluctuations for all life cycles, while life history strategies differed from each other in the extent of $\hat{n}_T$ reductions (fig. 4*b* for time $t < 100$; fig. 5*a*). The onset of gradual environmental change further reduced juvenile survival and evoked a decline in juvenile number and total population size (fig. 4*b*, 4*d* for time $t > 100$) before trait evolution allowed the population to adapt to the changing conditions (fig. 4*a*) and recover in a later phase of environmental change (fig. 4*d*). Evolutionary rescue resulted in a U-shaped curve in total population size n_T, with a population size recovery already occurring during environmental change or only after environmental change has stopped (fig. 4*b*).

Population Size Sensitivity to Environmental Variability. The sensitivity of the total population size $\hat{n}_T$ to environmental variance ϵ (fig. 5*a*, 5*b*) matched with our analytical expectations (see $\partial\hat{n}_T/\partial\bar{\sigma}_2$ values in table S1). The biennial two-stage life cycle (pre-sem, with precocious maturation

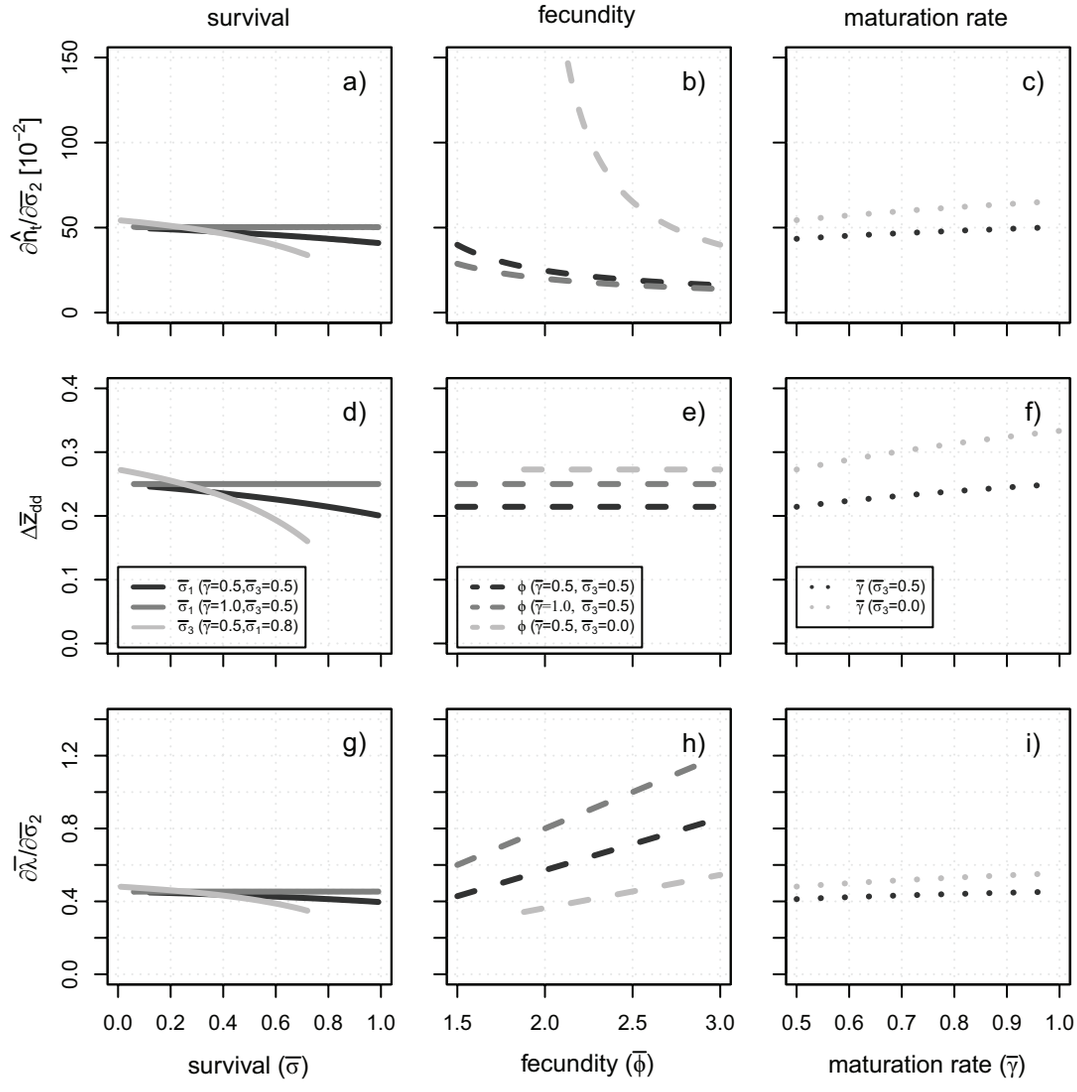

Figure 3: Shown are graphs illustrating the analytical results for the sensitivity of the total population size to juvenile survival ($\partial\hat{n}_T/\partial\bar{\sigma}_2 10^{-2}$; panels *a–c*), the rate of evolution ($\Delta\bar{z}_{dd}$; panels *d–f*), and the sensitivity of the population growth rate ($\partial\bar{\lambda}/\partial\bar{\sigma}_2$; panels *g–i*) for the three-stage life cycle depending on survival rate ($\bar{\sigma}_1$, $\bar{\sigma}_3$), fecundity ($\bar{\phi}$), and maturation probability ($\bar{\gamma}$). The sensitivity measures ($\partial\bar{\lambda}/\partial\bar{\sigma}_2$, $\partial\hat{n}_T/\partial\bar{\sigma}_2$) were estimated at equilibrium population size in the absence of interannual environmental variation at $\bar{\sigma}_2 = 0.8$. The maximum growth rate has been standardized for $\bar{\lambda}_{max} = 1.10$ by fecundity adjustments, except for the case with varying fecundity (panels *b*, *e*, *h*). Each parameter combination has been standardized for the same equilibrium population size in the absence of interannual environmental fluctuations ($\hat{n}_{Tmax} = 1{,}500$) via adjustments of the strength of competition (*b*). The rate of evolution was computed using equation (A23), the population size sensitivity was derived from equation (A11), and the growth rate sensitivity was calculated from explicit derivations from Mathematica. If not specified otherwise, the following parameter values were used: $\bar{\sigma}_1 = 0.8$, $\bar{\sigma}_3 = 0.5$, $\bar{\gamma} = 0.5$, $G_2 = 1$, and $\beta(\bar{z}_2) = 1$.

and semelparity) had the greatest sensitivity, shown in the decline of $\hat{n}_T$ with the strength of interannual environmental fluctuations (the variance ϵ; fig. 5*a*) and in the fluctuations of n_T over time (i.e., 90% quantile of total population size; fig. 5*b*). Sensitivity of $\hat{n}_T$ to fluctuations decreased among life histories as iteroparity ($\bar{\sigma}_3$) and maturation time ($1 - \bar{\gamma}$) increased (see table S1), from pre-sem to pre-ite, del-sem, and del-ite life histories. The standardization of the life histories for maximum growth rate $\bar{\lambda}_{max}$ did not affect the rank order of life history strategies (fig. S8). Overall, the sensitivity and the temporal fluctuations of n_T decreased when we increased $\bar{\lambda}_{max}$ from 1.10 to 1.15 (fig. 5*a*, 5*b*). A weaker strength of selection ($\omega^2 = 16$) also attenuated the sensitivity and stochasticity of population size for all life histories (fig. S9).

Rate of Directional Trait Evolution. As expected from our analytical predictions (table S1), the biennial life cycle

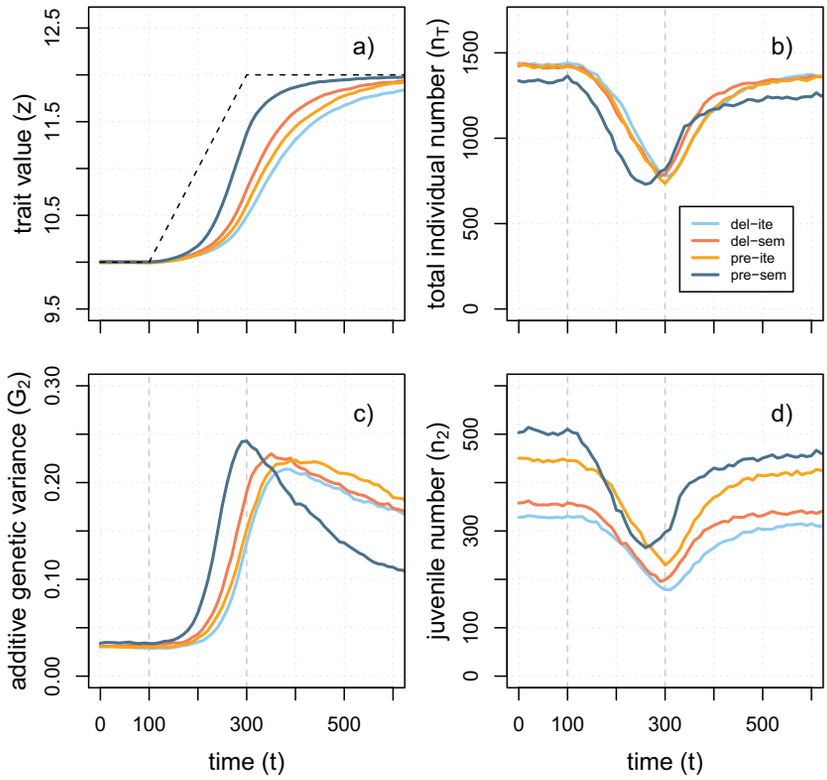

Figure 4: Shown are graphs illustrating the results of individual-based simulations for the mean trait value z (panel *a*), the total population size n_T (panel *b*), the additive genetic variance G_2 (panel *c*), and the juvenile number n_2 (panel *d*) for the four life histories (with delayed or precocious offspring maturation and semelparous or iteroparous adults; del-sem, del-ite, pre-ite, pre-sem) over 600 years. Environmental change started at $t = 100$ and was realized by a gradual shift in the phenotypic optimum (black dashed lines) from $\theta = 10$ to $\theta = 12$ by $t = 300$ (panel *a*). The between-year environmental fluctuations were set to variance $\epsilon = 0.2$, and life histories were standardized for $\bar{\lambda}_{max} = 1.15$. Average population sizes (n_T) were standardized to $\hat{n}_{Tmax} = 1{,}500$ in the absence of interannual environmental fluctuations and were depressed as a result of fitness reduction in juveniles from between-year fluctuations and directional environmental change (panel *b*). All values for total population size and trait values represent the arithmetic means over all of the 100 replicates that did not become extinct.

(pre-sem, with precocious maturation and semelparous adults) had the fastest evolutionary trait response to directional environmental change, while the del-ite life history with delayed maturation and iteroparity evolved the slowest (fig. 5*c*). However, even though the differences were small, species standardized for $\bar{\lambda}_{max} = 1.15$ evolved faster than species with $\bar{\lambda}_{max} = 1.10$ (fig. 5*c*), which was a deviation from the analytical predictions. Nevertheless, differences in evolvability were mainly found on a yearly absolute timescale. Once scaled to generation time, all life histories led to a similar number of generations to reach the same phenotypic threshold (fig. S8*c*).

Although standing genetic variation G_2 was similar across life history strategies after burn-in (fig. 5*d*), its temporal dynamics was strongly affected by the degree of iteroparity and delayed maturation—G_2 increased fastest during adaptation to new average local conditions in the pre-sem life cycle and slowest in the del-ite life cycle (fig. 4*c*). Overall, larger interannual fluctuations tended to increase standing genetic variation in all life histories as a result of greater fluctuating selection (fig. 5*d*).

Extinction Risk. The extinction risk of the population, evaluated as the total number of extinct replicates at a given time during the simulations (fig. 6), varied among life histories. In general, population extinctions were delayed relative to the onset of directional environmental change and still occurred after the environmental change stopped (fig. 6*a*, 6*c*). Life history strategies with high evolvability (e.g., pre-sem) led to earlier extinction because of larger demographic stochasticity leading to earlier declines in n_T than robust life histories (e.g., del-ite; fig. 4*b*, 4*d*). Life histories with high robustness (pre-ite, del-ite, del-sem; with delayed maturation and semelparous or iteroparous adults) caused larger extinction risks when we prolonged the period of environmental change from

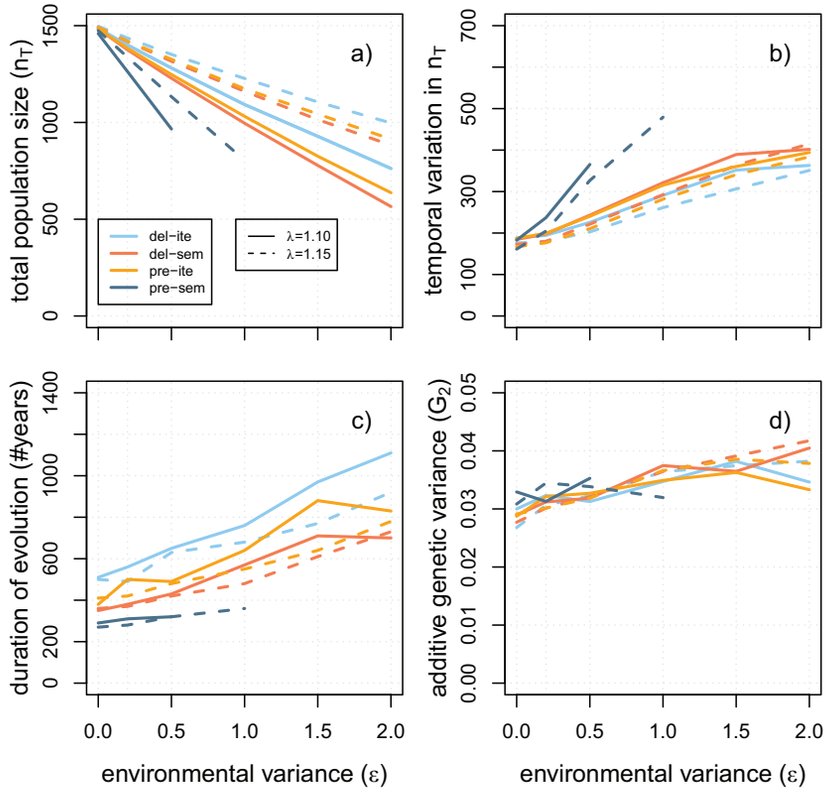

Figure 5: Shown are graphs illustrating the total population size n_T after burn-in (panel *a*), the variability in n_T over time (90% quantile of n_T over 500 years after burn-in; panel *b*), the speed of evolution (the average number of years to reach the trait value $z = 11.8$; panel *c*), and the standing genetic variance after burn-in (G_2; panel *d*) depending on the interannual environmental variability (ϵ). The simulation results are shown for four life histories with either precocious or delayed offspring maturation and semelparous or iteroparous adults (del-sem, del-ite, pre-ite, pre-sem) that have been standardized for two maximal population growth rates ($\bar{\lambda}_{max} = 1.10$, solid lines; $\bar{\lambda}_{max} = 1.15$, dashed lines) with environmental change lasting for 200 years. Note that the speed of evolution in panel *c* represents the arithmetic means over all of the 100 replicates that did not become extinct during environmental change. In contrast, the results for n_T (panel *a*), variability in n_T (panel *b*), and standing genetic variance G_2 (panel *d*) were averaged over all replicates, as no extinctions occurred after burn-in.

200 to 800 years, at least at low rates of random environmental fluctuations (fig. 6*c*). At high rates of interannual fluctuations, the biannual life cycle pre-sem always had the highest rate of extinction (fig. 6*b*, 6*d*). Overall, extinction risks were attenuated by having larger fecundity when setting $\bar{\lambda}_{max} = 1.15$ (fig. S10) and when reducing the strength of selection to $\omega^2 = 16$, where no extinction occurred (fig. S11).

Discussion

Life history strategies can impact a species' persistence in a dynamic environment, especially by helping it to cope with short-term interannual fluctuations and by shaping its evolutionary response to long-term gradual changes (Lande 1982; Hairston and De Stasio 1988; Barfield et al. 2011). In this study, we asked (i) whether a trade-off between a species' demographic robustness against environmental variability and its rate of trait evolution exists, (ii) how life history characteristics determine the position of a species along the robustness-evolvability trade-off, (iii) whether a genetic storage effect could alleviate the trade-off, and (iv) how the trade-off affects species persistence in fluctuating environments. Using existing theory from matrix population modeling and quantitative genetics, we confirmed numerically that a trade-off exists. However, current theory does not account for density-dependent population dynamics below carrying capacity and demographic feedback on the genetic variance of a population. For these reasons, we ran stochastic individual-based simulations. Here too we could confirm the hypothesized trade-off between a species' robustness and evolvability. Overall, we could show that along the fast-slow continuum, short-lived semelparous species had the fastest evolutionary response and could cope best with long-lasting directional environmental change but experienced the

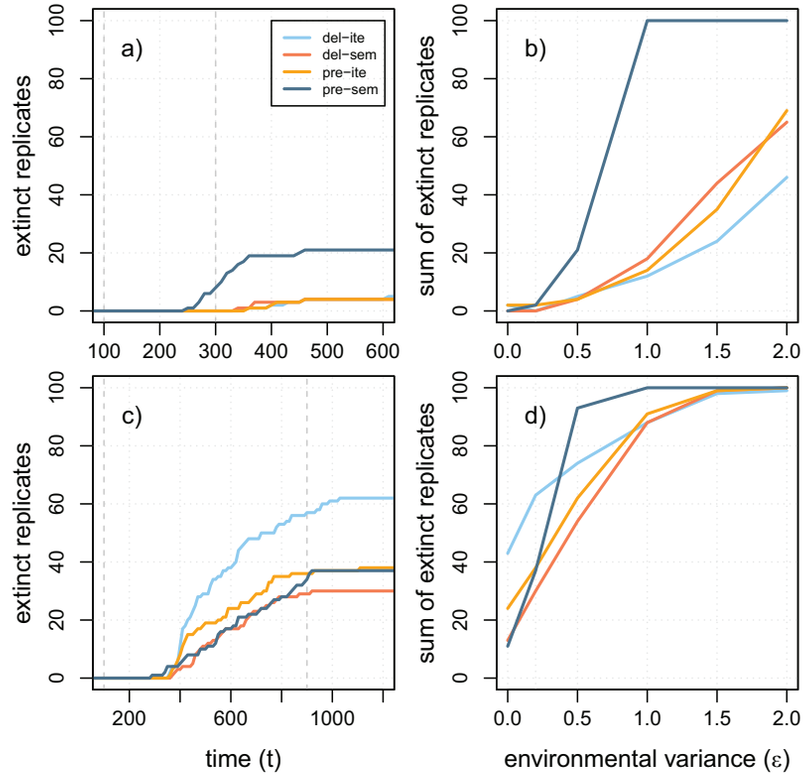

Figure 6: Shown are graphs illustrating the number of extinct replicates over time t (panels *a*, *c*) and the total number of extinct replicates depending on environmental variability ϵ (panels *b*, *d*) for each of the four life histories. Extinction dynamics are shown for two different scenarios with environmental change lasting either for 200 years (panels *a*, *b*) or for 800 years (panels *c*, *d*). The gray dashed lines indicate the start of environmental change ($t = 100$) and its end ($t = 300$ for panels *a*, *b*; $t = 900$ for panels *c*, *d*). In both scenarios, the rate of environmental change per year was set to $\Delta\bar{\theta} = 0.01$, and all life histories were standardized for a maximum growth rate of $\bar{\lambda}_{\max} = 1.10$. The temporal dynamics are shown for an environmental variability of $\epsilon = 0.5$ (panel *a*) and $\epsilon = 0.2$ (panel *c*).

highest extinction risk from interannual fluctuations and during the initial phase of environmental changes. They should thus suffer more from rapid anthropogenic climate changes than long-lived iteroparous species.

A higher robustness against random and uncorrelated between-year environmental fluctuations was achieved by three life history characteristics: offspring dormancy, higher adult survival (leading to iteroparity), and a larger maximum growth rate. Offspring dormancy and higher adult survival helped populations tolerate a variable environment by shielding a higher proportion of individuals from detrimental environmental conditions and spreading the risk of failed survival across years (e.g., see also Orzack and Tuljapurkar 1989; Tuljapurkar 1990; Koons et al. 2008; Zeineddine and Jansen 2009). In our simulations, offspring dormancy and iteroparity allowed the population to maintain larger sizes in the face of fluctuations while reducing its stochasticity in the total population density. In addition, a larger maximum growth rate improved the robustness to environmental variability by helping to recover faster from extreme events (see eq. [2] or Hallett et al. 2018).

In contrast to promoting robustness, evolvability benefited from shorter dormancy in offspring and reduced adult survival, both of which decreased generation time. Our models were calibrated to have constant equilibrium population sizes such that life histories with shorter generation times generally had a higher proportion of individuals in the juvenile stage (parameter w_3). Although the proportion of juveniles exposed to selection will affect the response to selection via the amount of additive genetic variation G_2 available for selection (i.e., the evolvability of the trait; see Houle 1992; Hansen and Houle 2008), the trait response also depends on the recruitment rate of selected juveniles (the product $\nu_3\bar{c}\sigma_2$; see, e.g., eq. [A18]). Higher recruitment improves the contribution of selected individuals to the next generation and increases the trait response (as shown in Barfield et al. 2011; see our eq. [5]). Simulations by Kuparinen et al. (2010) showed this effect when modeling the evolution of a quantitative trait in Scots pine and silver birch. A higher mortality in adult trees (e.g., from senescence or forest management) caused higher recruitment of juvenile trees (the only stage under selection)

and accelerated trait evolution in their simulations. This positive effect of juvenile recruitment on evolvability was also at work in our simulations, where higher juvenile recruitment was correlated with lower generation time. Higher recruitment and shorter generation time then favored the semelparous del-sem life cycle despite a lower proportion of juveniles exposed to selection over the iteroparous pre-ite life cycle with lower dormancy and a higher proportion of juveniles (see table S1; fig. 4).

In our simulations, the genetic storage effect did not affect the amount of standing genetic variation at the start of directional environmental change and did not help to overcome the trade-off between robustness and evolvability in long-lived species. Although all life histories led to the same level of standing genetic variation, they differed markedly in the evolution of additive genetic variance G_2 during environmental change. The genetic variance G_2 increased during directional selection in all simulations, as expected from the increase in allele frequencies of rare variants during adaptation toward a new trait optimum (Bürger 1999; Kopp and Matuszewski 2014) and the release of genetic variation caused by the Bulmer effect under stabilizing selection (i.e., switch from negative to positive genic covariance [linkage disequilibrium] when selection changes from stabilizing to directional; Bulmer 1971). This rise in G_2 happened most rapidly for the biennial life cycle (presem), with the highest proportion of individuals exposed to selection, and was slowest for the life history with offspring dormancy and iteroparity (del-ite). Likewise, additive genetic variance declined after a directional environmental change when selection became stabilizing again, with the fastest G_2 reductions in fast life histories. Life histories thus shaped the rate of evolution via G_2 differently from our initial expectations—in fact, in the opposite direction, such that the trade-off was not mitigated but enforced. Yet the storage effect has been shown to speed up evolution with overlapping generations for very large levels of environmental fluctuations (Yamamichi et al. 2019). However, we could not impose such high levels of environmental variance ϵ without driving populations to extinction when applying hard selection, while Yamamichi et al. (2019) simulated a yearly offspring production that was insensitive to ϵ.

To overcome the trade-off, a higher maximum growth rate could allow species to be more robust and at the same time more evolvable. In our models, a higher population growth rate $\bar{\lambda}_{\max}$ improved robustness against environmental fluctuations by helping to recover faster from detrimental environmental events and avoid extinction, in line with previous theory (Lynch and Lande 1993; Lande 1993; Bürger and Lynch 1995; Bürger 1999). Interestingly, a higher growth rate also caused faster trait evolution in our simulations, even though it had no or only very little effect on $\Delta\bar{z}$ in our mathematical models. Here, a higher $\bar{\lambda}_{\max}$, when realized by larger fecundity, was associated with more frequent mutation and recombination events. This effect of life history parameters on the amount of mutational input (fig. S12) is a process rarely accounted for in previous analytical models (but see Yamamichi et al. 2019) but should be of importance in natural systems. The effect of $\bar{\lambda}_{\max}$ further highlights the importance of standardizing life histories and making fair comparisons. Without a standardization of life histories for uniform $\bar{\lambda}_{\max}$ levels, one important way to overcome the trade-off could not have been identified.

The analytic evaluations and simulation results of this study were obtained assuming only one life stage under selection, even though the trade-off should still hold when multiple stages are sensitive to the environment, as suggested by equation (1). With multistage selection on a single trait, the growth rate sensitivities to multiple vital rates need to be considered, as do the covariances in environmental effects between stages (Tuljapurkar 1982; Tuljapurkar et al. 2009; Paniw et al. 2018). With a positive covariance in environmental effects, stage classes share positively correlated vital rate changes within a year and the same sign in the selection gradient during long-term environmental change. The exposure of multiple life stages to selection then should accelerate the rate of trait evolution (as a result of the sum with equally signed $\nabla_{\bar{z}_j}\bar{a}_{ij}$ values in eq. [8] of Barfield et al. 2011) but diminish demographic robustness (as implied by the additional reduction in the stochastic growth rate from a positive covariance in vital rate changes; Tuljapurkar 1982, p. 149). With a negative covariance in environmental effects, stage-specific selection gradients and fluctuations in vital rates oppose each other, thereby slowing down evolution but mitigating the demographic consequences of environmental fluctuations (Tuljapurkar 1982). As a consequence, life history strategies exposed to multistage selection still should face contrasting effects on evolvability and robustness and thus are limited by the same trade-off.

In conclusion, our results show that the feedback between evolutionary and demographic processes are critical for species persistence. A similar conclusion can be reached from models of evolutionary rescue (i.e., adaptation to single-shift environmental scenarios; Lynch et al. 1991; Lynch and Lande 1993; Bürger and Lynch 1995; Gomulkiewicz and Holt 1995; Gomulkiewicz and Houle 2009; Chevin 2013) or from models of species persistence on temporally shifting environmental gradients (i.e., models of species' range evolution; Polechová et al. 2009; Duputié et al. 2012). However, these models often ignore short-term perturbations (but see Orive et al. 2017), assume constant population growth (i.e., with density-independent growth; but see Boulding and Hay 2001), and do not incorporate explicit life cycles. On the other hand, quantitative

genetics models of trait evolution in stage-structured populations with (Engen et al. 2011, 2013) or without (Barfield et al. 2011) stochastic environmental fluctuations do not model species persistence, with a few recent exceptions (Marshall et al. 2016; Orive et al. 2017; Cotto et al. 2019). Importantly, no study to date explicitly addressed the trade-off between evolvability and demographic robustness. We have shown that such a trade-off exists and may limit the odds of evolutionary rescue in fast life histories. Slow life histories may persist longer while accumulating large adaptation lags, experiencing delayed population declines, and facing extinction debts (Dullinger et al. 2012; Cotto et al. 2017).

Implications. We highlighted a fundamental property of eco-evolutionary dynamics whereby a larger evolutionary response comes at the expense of a lower demographic robustness to variation in vital rates in populations adapting to a fluctuating environment. Our conclusions are based on comparisons of eco-evolutionary dynamics of standardized life cycles. However, life history strategies in natural systems are not standardized. In fact, systematic differences in more than one life history characteristic exist. Species with low generation times often exhibit systematically higher population sizes ($\hat{n}_T$), greater intrinsic growth rates, larger dispersal abilities, and lower competitive abilities than species with long generation times (Petit and Hampe 2006; Buoro and Carlson 2014; Beckman et al. 2018). They might thus be more robust to changes than predicted here. Similarly, long-lived species may suffer more from climate changes if adult mortality is increased, reducing their robustness but increasing their evolvability. For instance, adult trees may be sensitive to extreme weather events, such as drought or forest fires (e.g., Van Mantgem and Stephenson 2007). By simplifying the action of selection on a single life stage (e.g., on tree seedlings), we have not incorporated possible feedback between environmentally induced selection and life history characteristics. Such feedback could change the life history of the species, as shown by Cotto et al. (2019), and move the species along the fast-slow life history trade-off between evolvability and robustness. Instead, we have characterized archetype life history strategies that span the fast-slow continuum and exemplified possible outcomes arising from the trade-off. Our work thus shows the importance of merging population ecology with evolutionary quantitative genetics in a dynamical and stochastic modeling framework to characterize species' vulnerability to environmental changes.

Acknowledgments

We thank Thomas F. Hansen, Luis-Miguel Chevin, Olivier Cotto, Laurence D. Mueller, and, in particular, Richard Gomulkiewicz for insightful discussions and comments on the manuscript. We are also grateful to six anonymous reviewers and the editors for their detailed comments on the manuscript. M.S. and F.G. were supported by grants PP00P3_144846 and PP00P3_176965 from the Swiss National Science Foundation to F.G. The authors declare no conflicts of interest.

Statement of Authorship

M.S. and F.G. conceived the study, and all authors further developed the approach. M.S. and F.G. derived the mathematical equations. M.S. performed the simulations and analyzed output data. M.S. and F.G. wrote the manuscript. All authors substantially contributed to revisions of early drafts of this work.

Data and Code Availability

Data and code for the simulations are available in the Dryad Digital Repository (https://doi.org/10.5061/dryad.hx3ffbgdv; Schmid et al. 2022). The release version of Nemo for stage-structured populations can be found at https://bitbucket.org/ecoevo/nemo-age-release/src/master/.

APPENDIX A

Three-Stage Model

Equilibrium Population Size

The populations' demographic dynamics were modeled via the population vector

$$N = \begin{pmatrix} n_1 \\ n_2 \\ n_3 \end{pmatrix} \tag{A1}$$

and the MPM

$$A = \begin{bmatrix} \bar{\sigma}_1(1-\bar{\gamma}) & 0 & \bar{\phi} \\ \bar{\sigma}_1(\bar{\gamma}) & 0 & 0 \\ 0 & \bar{\sigma}_2 \exp(-bn_3) & \bar{\sigma}_3 \end{bmatrix}, \tag{A2}$$

such that $N(t+1) = AN(t)$. By solving for the stage densities at equilibrium when $\hat{N} = A\hat{N}$, with $\hat{N} = (\hat{n}_1, \hat{n}_2, \hat{n}_3)^T$, the individual numbers within the offspring, juvenile, and adult stages at equilibrium could be derived as

$$\hat{n}_1 = \frac{\bar{\phi}}{b(\bar{\sigma}_1(1-\bar{\gamma})-1)} \times \log\left(\frac{(1+\bar{\sigma}_1\bar{\gamma}-\bar{\sigma}_1)(1-\bar{\sigma}_3)}{\bar{\phi}\bar{\sigma}_1\bar{\gamma}\bar{\sigma}_2}\right), \tag{A3}$$

$$\hat{n}_2 = \frac{\bar{\phi}\bar{\sigma}_1\bar{\gamma}}{b(\bar{\sigma}_1(1-\bar{\gamma})-1)} \times \log\left(\frac{(1+\bar{\sigma}_1\bar{\gamma}-\bar{\sigma}_1)(1-\bar{\sigma}_3)}{\bar{\phi}\bar{\sigma}_1\bar{\gamma}\bar{\sigma}_2}\right), \tag{A4}$$

$$\hat{n}_3 = \frac{1}{-b} \times \log\left(\frac{(1+\bar{\sigma}_1\bar{\gamma}-\bar{\sigma}_1)(1-\bar{\sigma}_3)}{\bar{\phi}\bar{\sigma}_1\bar{\gamma}\bar{\sigma}_2}\right). \tag{A5}$$

The total population size at equilibrium was computed from $\hat{n}_T = \hat{n}_1 + \hat{n}_2 + \hat{n}_3$ as

$$\hat{n}_t = \frac{\bar{\phi}+\bar{\sigma}_1\bar{\gamma}(\bar{\phi}+1)-\bar{\sigma}_1+1}{b(\bar{\sigma}_1(1-\bar{\gamma})-1)} \times \log\left(\frac{(1+\bar{\sigma}_1\bar{\gamma}-\bar{\sigma}_1)(1-\bar{\sigma}_3)}{\bar{\phi}\bar{\sigma}_1\bar{\gamma}\bar{\sigma}_2}\right). \tag{A6}$$

Sensitivity of Total Population Size to Juvenile Survival

The partial derivative of the total population size at equilibrium ($\hat{n}_T$) to juvenile survival ($\bar{\sigma}_2$) was calculated as

$$\frac{\partial\hat{n}_T}{\partial\bar{\sigma}_2} = \frac{\bar{\phi}+\bar{\sigma}_1\bar{\gamma}(\bar{\phi}+1)-\bar{\sigma}_1+1}{b(\bar{\sigma}_1(1-\bar{\gamma})-1)} \times \frac{\bar{\phi}\bar{\sigma}_1\bar{\gamma}\bar{\sigma}_2}{(1+\bar{\sigma}_1\bar{\gamma}-\bar{\sigma}_1)(1-\bar{\sigma}_3)} \times \left(\frac{-1\bar{\phi}\bar{\sigma}_1\bar{\gamma}(1+\bar{\sigma}_1\bar{\gamma}-\bar{\sigma}_1)(1-\bar{\sigma}_3)}{(\bar{\phi}\bar{\sigma}_1\bar{\gamma}\bar{\sigma}_2)^2}\right), \tag{A7}$$

which could be simplified to

$$\frac{\partial\hat{n}_T}{\partial\bar{\sigma}_2} = \frac{\bar{\sigma}_1(1-\bar{\gamma})-1-\bar{\phi}(1+\bar{\sigma}_1\bar{\gamma})}{b\bar{\sigma}_2(\bar{\sigma}_1(1-\bar{\gamma})-1)}. \tag{A8}$$

To reach equal $\bar{\lambda}_{max}$ across life histories, we adjusted the fecundity $\bar{\phi}$ using a numeric approach (i.e., by iterations of the lambda function in the popbio package in R; Stubben and Milligan 2007; R Core Team 2019). To standardize a life history for a specific total equilibrium population size ($\hat{n}_{T\,max}$), the strength of intraspecific competition was adjusted as follows:

$$b = \frac{\bar{\phi}+\bar{\sigma}_1\bar{\gamma}(\bar{\phi}+1)-\bar{\sigma}_1+1}{\hat{n}_{T\,max}(\bar{\sigma}_1(1-\bar{\gamma})-1)} \times \log\left(\frac{(1+\bar{\sigma}_1\bar{\gamma}-\bar{\sigma}_1)(1-\bar{\sigma}_3)}{\bar{\phi}\bar{\sigma}_1\bar{\gamma}\bar{\sigma}_2}\right). \tag{A9}$$

By inserting equation (A9) into equation (A8), the population size sensitivity can be expressed depending on the equilibrium population size as

$$\frac{\partial\hat{n}_T}{\partial\bar{\sigma}_2} = \frac{\bar{\sigma}_1(1-\bar{\gamma})-1-\bar{\phi}(1+\bar{\sigma}_1\bar{\gamma})}{\bar{\sigma}_2(\bar{\sigma}_1(1-\bar{\gamma})-1)} \times \frac{\hat{n}_{T\,max}(\bar{\sigma}_1(1-\bar{\gamma})-1)}{\bar{\phi}+\bar{\sigma}_1\bar{\gamma}(\bar{\phi}+1)-\bar{\sigma}_1+1} \times \log\left(\frac{(1+\bar{\sigma}_1\bar{\gamma}-\bar{\sigma}_1)(1-\bar{\sigma}_3)}{\bar{\phi}\bar{\sigma}_1\bar{\gamma}\bar{\sigma}_2}\right)^{-1}, \tag{A10}$$

such that the partial derivative

$$\frac{\partial\hat{n}_T}{\partial\bar{\sigma}_2} = \frac{-\hat{n}_{T\,max}}{\bar{\sigma}_2} \times \log\left(\frac{(1+\bar{\sigma}_1\bar{\gamma}-\bar{\sigma}_1)(1-\bar{\sigma}_3)}{\bar{\phi}\bar{\sigma}_1\bar{\gamma}\bar{\sigma}_2}\right)^{-1} \tag{A11}$$

is obtained and simplified to

$$\frac{\partial\hat{n}_T}{\partial\bar{\sigma}_2} = \frac{-\hat{n}_{T\,max}}{\bar{\sigma}_2\log(\bar{c})}, \tag{A12}$$

with the probability of surviving intraspecific competition $\bar{c}$ (see eq. [A20]).

Rate of Evolution with Exponential Growth

We adapted equation (8) from Barfield et al. (2011) for our three-stage life cycle in the absence of density regulation. In Barfield et al. (2011), the rate of evolution ($\Delta\bar{z}$) is described as a function of the additive genetic variance (G), the average growth rate ($\bar{\lambda}$), average vital rates ($\bar{a}_{ij}$), the stable population structure (w), stage-specific reproductive values (v), and the gradient operator with respect to trait means ($\nabla_{\bar{z}_j}$). We assume that the vital rate of juveniles can be expressed as $\bar{a}_{32} = \sigma_{2\,max}\bar{W}(\bar{z}_2)$, the product of maximum juvenile survival σ_{2max} and average juvenile survival depending on the match between phenotype and environment $\bar{W}(\bar{z}_2)$. Then, with $\bar{a}_{32}\partial\ln(\bar{a}_{32})/\partial\bar{z}_2 = \sigma_{2\,max}\bar{W}(\bar{z}_2)\partial\ln(\bar{W}(\bar{z}_2))/\partial\bar{z}_2$ and writing $\beta(\bar{z}_2) = \partial\ln(\bar{W}(\bar{z}_2))/\partial\bar{z}_2$ (Lande 1979; Lande and Arnold 1983) as well as $\bar{\sigma}_2 = \sigma_{2\,max}\bar{W}(\bar{z}_2)$, the asymptotic rate of evolution is

$$\Delta\bar{z}_{exp} = \frac{1}{\bar{\lambda}}v_3w_2\bar{\sigma}_2G_2\beta(\bar{z}_2). \tag{A13}$$

The juvenile proportion (w_2) could be derived from the right eigenvector of A (Caswell 2001, p. 87) when solving $Aw = \bar{\lambda}w$ as

$$w_2 = \frac{\bar{\sigma}_1\bar{\gamma}(\bar{\lambda}-\bar{\sigma}_3)}{\bar{\lambda}(\bar{\lambda}-\bar{\sigma}_3)+\bar{\sigma}_1\bar{\gamma}(\bar{\lambda}-\bar{\sigma}_3)+\bar{\sigma}_1\bar{\gamma}\bar{\sigma}_2}. \tag{A14}$$

The reproductive value of adults (v_3) could be derived from the left eigenvector (v) of A when solving $v^TA = \bar{\lambda}v^T$ (Caswell 2001, eq. [4.81]) as

$$v_3 = \frac{\bar{\lambda}(\bar{\lambda} - \bar{\sigma}_1(1-\bar{\gamma}))}{\bar{\sigma}_2\bar{\sigma}_1\bar{\gamma}} \tag{A15}$$

and normalized to

$$v_3 = \frac{\bar{\lambda}(\bar{\lambda} - \bar{\sigma}_1(1-\bar{\gamma}))}{\bar{\sigma}_2\bar{\sigma}_1\bar{\gamma}} \times \frac{\bar{\lambda}(\bar{\lambda}-\bar{\sigma}_3) + \bar{\sigma}_1\bar{\gamma}(\bar{\lambda}-\bar{\sigma}_3) + \bar{\sigma}_2\bar{\sigma}_1\bar{\gamma}}{\bar{\lambda}(\bar{\lambda}-\bar{\sigma}_3) + (\bar{\lambda}-\bar{\sigma}_3)(\bar{\lambda}-\bar{\sigma}_1(1-\bar{\gamma})) + \bar{\lambda}(\bar{\lambda}-\bar{\sigma}_1(1-\bar{\gamma}))}, \tag{A16}$$

such that $v^{\mathrm{T}}w = 1$ (as in Barfield et al. 2011). The rate of evolution depending on $\bar{\lambda}$ becomes:

$$\Delta\bar{z}_{\mathrm{exp}} = \frac{(\bar{\lambda}-\bar{\sigma}_3)(\bar{\lambda}-\bar{\sigma}_1(1-\bar{\gamma}))}{(\bar{\lambda}-\bar{\sigma}_3)(\bar{\lambda}-\bar{\sigma}_1(1-\bar{\gamma})) + \bar{\lambda}(\bar{\lambda}-\bar{\sigma}_3) + \bar{\lambda}(\bar{\lambda}-\bar{\sigma}_1(1-\bar{\gamma}))} G_2\beta(\bar{z}_2). \tag{A17}$$

Note that with exponential growth, the growth rate $\bar{\lambda}$ here corresponds to the maximum growth rate $\bar{\lambda}_{\max}$ (= in absence of density regulation) as mentioned in the main text.

Rate of Evolution at Equilibrium Population Size

With density-dependent population growth, we assume that the rate of evolution can be approximated from the Lande theorem as well (Barfield et al. 2011, eq. [8]), at least in the absence of density-dependent selection when the population reaches equilibrium density ($\bar{\lambda} = 1$) and when population dynamics are faster than evolutionary dynamics. Then, competition survival $\bar{c}$ and the transition matrix A are nearly constant over time and the population reaches SSD while not being at the phenotypic optimum yet. Thereby, all assumptions to solve equation (B2) in Barfield et al. (2011) are met. Furthermore, the growth rate sensitivity ($\partial\bar{\lambda}/\partial\bar{\sigma}_2$) of both models, with exponential growth and at equilibrium population size, is then equivalent (see fig. S13).

We assume that the vital rate of juveniles can be expressed as $\bar{a}_{32} = \bar{c}\sigma_{2\max}\bar{W}(\bar{z}_2)$, the product of maximum juvenile survival $\sigma_{2\max}$, average juvenile survival depending on the match between phenotype and environment $\bar{W}(\bar{z}_2)$, and competition survival $\bar{c}$. Then, with $\bar{a}_{32}\partial\ln(\bar{a}_{32})/\partial\bar{z}_2 = \sigma_{2\max}\bar{W}(\bar{z}_2)c\partial\ln(\bar{W}(\bar{z}_2))/\partial\bar{z}_2$ and writing $\beta(\bar{z}_2) = \partial\ln(\bar{W}(\bar{z}_2))/\partial\bar{z}_2$ (Lande 1979; Lande and Arnold 1983) as well as $\bar{\sigma}_2 = \sigma_{2\max}\bar{W}(\bar{z}_2)$, the asymptotic rate of evolution is equal to

$$\Delta\bar{z}_{\mathrm{dd}} = v_3 w_2 \bar{c}\bar{\sigma}_2 G_2\beta(\bar{z}_2). \tag{A18}$$

The juvenile proportion (w_2) could be derived from equations (A4) and (A6) as

$$w_2 = \frac{\hat{n}_2}{\hat{n}_{\mathrm{T}}} = \frac{\bar{\phi}\bar{\sigma}_1\bar{\gamma}}{\bar{\phi} + \bar{\sigma}_1\bar{\gamma}(\bar{\phi}+1) - \bar{\sigma}_1 + 1}. \tag{A19}$$

The probability of surviving intraspecific competition ($\bar{c}$) was derived by combining the Ricker function $\bar{c} = \exp(-bn_3)$ and equation (A5) as

$$\bar{c} = \frac{(1-\bar{\sigma}_3)(1+\bar{\sigma}_1\bar{\gamma}-\bar{\sigma}_1)}{\bar{\phi}\bar{\sigma}_1\bar{\gamma}\bar{\sigma}_2}. \tag{A20}$$

The reproductive value of adults (v_3) could be derived from the left eigenvector (v of the MPM (A) when solving $vA = \bar{\lambda}v$ (Caswell 2001, eq. [4.81]). For a population at equilibrium population size ($\bar{\lambda} = 1$), the reproductive value of adults can be derived as

$$v_3 = \frac{\bar{\phi}}{(1-\bar{\sigma}_3)} \tag{A21}$$

and normalized to

$$v_3 = \frac{\bar{\phi} + \bar{\sigma}_1\bar{\gamma}(\bar{\phi}+1) - \bar{\sigma}_1 + 1}{(1-\bar{\sigma}_3)(1-\bar{\sigma}_1(1-\bar{\gamma})) + (1-\bar{\sigma}_3) + (1-\bar{\sigma}_1(1-\bar{\gamma}))}, \tag{A22}$$

such that $v^{\mathrm{T}}w = 1$ (as in Barfield et al. 2011). The rate of evolution at equilibrium population density ($\bar{\lambda} = 1$) becomes

$$\Delta\bar{z}_{\mathrm{dd}} = \frac{(1-\bar{\sigma}_3)(1-\bar{\sigma}_1(1-\bar{\gamma}))}{(1-\bar{\sigma}_3)(1-\bar{\sigma}_1(1-\bar{\gamma})) + (1-\bar{\sigma}_3) + (1-\bar{\sigma}_1(1-\bar{\gamma}))} G_2\beta(\bar{z}_2). \tag{A23}$$

APPENDIX B

Two-Stage Model

Equilibrium Population Size

The demographic dynamics for a two-stage life history with nonoverlapping generations were modeled by the population vector

$$N = \begin{pmatrix} n_2 \\ n_3 \end{pmatrix} \tag{B1}$$

and the MPM

$$A = \begin{bmatrix} 0 & \bar{\phi} \\ \bar{\sigma}_2\exp(-bn_2) & 0 \end{bmatrix}, \tag{B2}$$

such that $N(t+1) = AN(t)$. By solving for the individual numbers within stages at equilibrium when $\hat{N} = A\hat{N}$ and $\hat{N} = (\hat{n}_2, \hat{n}_3)^{\mathrm{T}}$, the juvenile and adult numbers at equilibrium were derived as

$$\hat{n}_2 = \frac{-\bar{\phi}}{b\bar{\phi}} \log\left(\frac{1}{\bar{\phi}\bar{\sigma}_2}\right), \tag{B3}$$

$$\hat{n}_3 = \frac{-1}{b\bar{\phi}} \log\left(\frac{1}{\bar{\phi}\bar{\sigma}_2}\right) \tag{B4}$$

(with natural logarithm log()). The total population size at equilibrium was computed from $\hat{n}_T = \hat{n}_2 + \hat{n}_3$ as

$$\hat{n}_T = \frac{-1 - \bar{\phi}}{b\bar{\phi}} \log\left(\frac{1}{\bar{\phi}\bar{\sigma}_2}\right). \tag{B5}$$

Sensitivity of Total Population Size to Juvenile Survival

The partial derivative of the total population size at equilibrium $\hat{n}_T$ to juvenile survival $\bar{\sigma}_2$ was derived as

$$\frac{\partial \hat{n}_T}{\partial \bar{\sigma}_2} = \frac{(-\bar{\phi} - 1)}{b\bar{\phi}} \frac{\bar{\sigma}_2\bar{\phi}}{1} \frac{-\bar{\phi}}{\bar{\phi}^2\bar{\sigma}_2^2}, \tag{B6}$$

which could be simplified to

$$\frac{\partial \hat{n}_T}{\partial \bar{\sigma}_2} = \frac{(\bar{\phi} + 1)}{b\bar{\sigma}_2\bar{\phi}}. \tag{B7}$$

To reach a certain total equilibrium population size ($\hat{n}_{T\max}$), the strength of intraspecific competition (b) was standardized as follows:

$$b = \frac{-1 - \bar{\phi}}{\hat{n}_{T\max}\bar{\phi}} \log\left(\frac{1}{\bar{\phi}\bar{\sigma}_2}\right). \tag{B8}$$

Given that the maximum growth rate $\bar{\lambda}_{\max}$ could be calculated from

$$\bar{\lambda}_{\max} = \sqrt{\bar{\sigma}_2\bar{\phi}}, \tag{B9}$$

when density dependence is absent ($\bar{c} = 1$ when $n_2 = 0$), life histories could be standardized for $\bar{\lambda}_{\max}$ via $\bar{\phi}$ adjustments as

$$\bar{\phi} = \frac{\bar{\lambda}_{\max}^2}{\bar{\sigma}_2}, \tag{B10}$$

such that the sensitivity $\partial \hat{n}_T / \partial \bar{\sigma}_2$ could be generalized to

$$\frac{\partial \hat{n}_T}{\partial \bar{\sigma}_2} = \frac{-n_{T\max}}{\bar{\sigma}_2} \log\left(\frac{1}{\bar{\lambda}_{\max}^2}\right)^{-1}. \tag{B11}$$

Rate of Evolution with Exponential Growth

To describe the rate of evolution, we adapted equation (8) from Barfield et al. (2011) for our two-stage life cycle similar to the three-stage life history as

$$\Delta\bar{z}_{\exp} = \frac{1}{\bar{\lambda}} v_3 w_2 \bar{\sigma}_2 G_2 \beta(\bar{z}_2). \tag{B12}$$

The proportion of juveniles (w_2) could be derived from the right eigenvector of A as

$$w_2 = \frac{\bar{\sigma}_2}{\bar{\lambda} + \bar{\sigma}_2}. \tag{B13}$$

The reproductive value of adults (v_3) could be derived from the left eigenvector (v) of A as

$$v_3 = \frac{\bar{\lambda}}{\bar{\sigma}_2} \tag{B14}$$

and normalized to

$$v_3 = \frac{\bar{\lambda} + \sigma_2}{2\bar{\sigma}_2}, \tag{B15}$$

such that $v^T w = 1$ (as in Barfield et al. 2011). The rate of evolution depending on the single vital rates then could be expressed as

$$\Delta\bar{z}_{\exp} = \frac{1}{2} G_2 \beta(\bar{z}_2). \tag{B16}$$

Rate of Evolution at Equilibrium Population Size

To describe the rate of evolution at carrying capacity ($\bar{\lambda} = 1$), we adapted equation (8) from Barfield et al. (2011) for our two-stage life cycle similar to the three-stage life history as

$$\Delta\bar{z}_{dd} = \frac{1}{\bar{\lambda}} v_3 w_2 \bar{c} \bar{\sigma}_2 G_2 \beta(\bar{z}_2). \tag{B17}$$

The juvenile proportion could be derived from equations (B3) and (B5):

$$w_2 = \frac{\hat{n}_2}{\hat{n}_T} = \frac{\bar{\phi}}{1 + \bar{\phi}}. \tag{B18}$$

The probability of surviving intraspecific competition (c) was derived by combining the Ricker function $\bar{c} = \exp(-bn_2)$ and equation (B3):

$$\bar{c} = \exp(-bn_2) = \frac{1}{\bar{\phi}\sigma_2}. \tag{B19}$$

The reproductive value of adults (v_3) could be derived from the left eigenvector (v) of the MPM (A) when solving $vA = \bar{\lambda}v$ (Caswell 2001, eq. [4.81]). For a population at equilibrium ($\bar{\lambda} = 1$), the reproductive value of adults could be derived as

$$v_3 = \bar{\phi} \tag{B20}$$

and normalized to

$$v_3 = \frac{1 + \bar{\phi}}{2}, \tag{B21}$$

such that $v^T w = 1$ (as in Barfield et al. 2011). The rate of evolution depending on the single vital rates could then be expressed as

$$\Delta\bar{z}_{\mathrm{dd}} = \frac{1}{2} G_2 \beta(\bar{z}_2). \tag{B22}$$

Literature Cited

Aitken, S. N., S. Yeaman, J. A. Holliday, T. Wang, and S. Curtis-McLane. 2008. Adaptation, migration or extirpation: climate change outcomes for tree populations. Evolutionary Applications 1:95–111.

Barfield, M., R. D. Holt, and R. Gomulkiewicz. 2011. Evolution in stage-structured populations. American Naturalist 177:397–409.

Beckman, N., J. M. Bullock, and R. Salguero-Gómez. 2018. High dispersal ability is related to fast life history strategies. Journal of Ecology 106:1349–1362.

Bell, G., and A. Gonzalez. 2009. Evolutionary rescue can prevent extinction following environmental change. Ecology Letters 12:942–948.

Boulding, E. G., and T. Hay. 2001. Genetic and demographic parameters determining population persistence after a discrete change in the environment. Heredity 86:313–324.

Boyce, M. S., C. V. Haridas, C. T. Lee, C. L. Boggs, E. M. Bruna, T. Coulson, D. Doak, et al. 2006. Demography in an increasingly variable world. Trends in Ecology and Evolution 21:141–148.

Bulmer, M. G. 1971. The effect of selection on genetic variability. American Naturalist 105:201–211.

Buoro, M., and S. M. Carlson. 2014. Life-history syndromes: integrating dispersal through space and time. Ecology Letters 17:756–767.

Bürger, R. 1999. Evolution of genetic variability and the advantage of sex and recombination in changing environments. Genetics 153:1055–1069.

Bürger, R., and M. Lynch. 1995. Evolution and extinction in a changing environment: a quantitative-genetic analysis. Evolution 49:151–163.

Carlson, S. M., C. J. Cunningham, and P. A. Westley. 2014. Evolutionary rescue in a changing world. Trends in Ecology and Evolution 29:521–530.

Caswell, H. 2001. Matrix population models: construction, analysis, and interpretation. 2nd ed. Sinauer, Sunderland, MA.

Caswell, H., T. Takada, and C. M. Hunter. 2004. Sensitivity analysis of equilibrium in density-dependent matrix population models. Ecology Letters 7:380–387.

Cayuela, H., P. Joly, B. R. Schmidt, J. Pichenot, E. Bonnaire, P. Priol, O. Peyronel, M. Laville, and A. Besnard. 2017. Life history tactics shape amphibians' demographic responses to the North Atlantic Oscillation. Global Change Biology 23:4620–4638.

Charlesworth, B. 1994. Evolution in age-structured populations. 2nd ed. Cambridge University Press, Cambridge.

Chevin, L.-M. 2013. Genetic constraints on adaptation to a changing environment. Evolution 67:708–721.

Chevin, L.-M., O. Cotto, and J. Ashander. 2017. Stochastic evolutionary demography under a fluctuating optimum phenotype. American Naturalist 190:786–802.

Cohen, D. 1967. Optimizing reproduction in a randomly varying environment when a correlation may exist between the conditions at the time a choice has to be made and the subsequent outcome. Journal of Theoretical Biology 16:1–14.

Cotto, O., L. Sandell, L.-M. Chevin, and O. Ronce. 2019. Maladaptive shifts in life history in a changing environment. American Naturalist 194:558–573.

Cotto, O., M. Schmid, and F. Guillaume. 2020. Nemo-age: spatially explicit simulations of eco-evolutionary dynamics in stage-structured populations under changing environments. Methods in Ecology and Evolution 11:1227–1236.

Cotto, O., J. Wessely, D. Georges, G. Klonner, M. Schmid, S. Dullinger, W. Thuiller, and F. Guillaume. 2017. A dynamic eco-evolutionary model predicts slow response of alpine plants to climate warming. Nature Communications 8:15399.

Dalgleish, H. J., D. N. Koons, and P. B. Adler. 2010. Can life-history traits predict the response of forb populations to changes in climate variability? Journal of Ecology 98:209–217.

Doak, D. F., and W. F. Morris. 2010. Demographic compensation and tipping points in climate-induced range shifts. Nature 467:959–962.

Dullinger, S., A. Gattringer, W. Thuiller, D. Moser, N. E. Zimmermann, A. Guisan, W. Willner, et al. 2012. Extinction debt of high-mountain plants under twenty-first-century climate change. Nature Climate Change 2:619–622.

Duputié, A., F. Massol, I. Chuine, M. Kirkpatrick, and O. Ronce. 2012. How do genetic correlations affect species range shifts in a changing environment? Ecology Letters 15:251–259.

Duputié, A., A. Rutschmann, O. Ronce, and I. Chuine. 2015. Phenological plasticity will not help all species adapt to climate change. Global Change Biology 21:3062–3073.

Ellner, S. P., and N. G. Hairston. 1994. Role of overlapping generations in maintaining genetic variation in a fluctuating environment. American Naturalist 143:403–417.

Engen, S., R. Lande, and B.-E. Saether. 2009. Reproductive value and fluctuating selection in an age-structured population. Genetics 183:629–637.

———. 2011. Evolution of a plastic quantitative trait in an age-structured population in a fluctuating environment. Evolution 65:2893–2906.

———. 2013. A quantitative genetic model of *r*- and *K*-selection in a fluctuating population. American Naturalist 181:725–736.

Engen, S., R. Lande, B.-E. Sæther, and H. Weimerskirch. 2005. Extinction in relation to demographic and environmental stochasticity in age-structured models. Mathematical Biosciences 195:210–227.

Evans, M. E. K., and J. J. Dennehy. 2005. Germ banking: bet-hedging and variable release from egg and seed dormancy. Quarterly Review of Biology 80:431–451.

Gaillard, J.-M., D. Pontier, D. Allainé, J. D. Lebreton, J. Trouvilliez, and J. Clobert. 1989. An analysis of demographic tactics in birds and mammals. Oikos 56:59–76.

Gaillard, J.-M., N. G. Yoccoz, J. Lebreton, C. Bonenfant, S. Devillard, A. Loison, D. Pontier, and D. Allaine. 2005. Generation time: a reliable metric to measure life-history variation among mammalian populations. American Naturalist 166:119–123.

Gomulkiewicz, R., and R. D. Holt. 1995. When does evolution by natural selection prevent extinction? Evolution 49:201–207.

Gomulkiewicz, R., and D. Houle. 2009. Demographic and genetic constraints on evolution. American Naturalist 174:E218–E229.

Grant, A., and T. G. Benton. 2000. Elasticity analysis for density-dependent populations in stochastic environments. Ecology 81:680–693.

———. 2003. Density-dependent populations require density-dependent elasticity analysis: an illustration using the LPA model of *Tribolium*. Journal of Animal Ecology 72:94–105.

Guillaume, F., and J. Rougemont. 2006. Nemo: an evolutionary and population genetics programming framework. Bioinformatics 22:2556–2557.

Hairston, N. G., and B. T. De Stasio Jr. 1988. Rate of evolution slowed by a dormant propagule pool. Nature 336:239–242.

Hallett, L. M., E. C. Farrer, K. N. Suding, H. A. Mooney, and R. J. Hobbs. 2018. Tradeoffs in demographic mechanisms underlie differences in species abundance and stability. Nature Communications 9:1–6.

Hansen, T. F., and D. Houle. 2008. Measuring and comparing evolvability and constraint in multivariate characters. Journal of Evolutionary Biology 21:1201–1219.

Hansen, T. F., T. M. Solvin, and M. Pavlicev. 2019. Predicting evolutionary potential: a numerical test of evolvability measures. Evolution 73:689–703.

Houle, D. 1992. Comparing evolvability and variability of quantitative traits. Genetics 130:195–204.

Koons, D. N., C. J. E. Metcalf, and S. Tuljapurkar. 2008. Evolution of delayed reproduction in uncertain environments: a life-history perspective. American Naturalist 172:797–805.

Kopp, M., and S. Matuszewski. 2014. Rapid evolution of quantitative traits: theoretical perspectives. Evolutionary Applications 7:169–191.

Kuparinen, A., O. Savolainen, and F. M. Schurr. 2010. Increased mortality can promote evolutionary adaptation of forest trees to climate change. Forest Ecology and Management 259:1003–1008.

Lande, R. 1979. Quantitative genetic analysis of multivariate evolution, applied to brain : body size allometry. Evolution 33:402–416.

———. 1982. A quantitative genetic theory of life history evolution. Ecology 63:607–615.

———. 1993. Risks of population extinction from demographic and environmental stochasticity and random catastrophes. American Naturalist 142:911–927.

———. 2007. Expected relative fitness and the adaptive topography of fluctuating selection. Evolution 61:1835–1846.

Lande, R., and S. J. Arnold. 1983. The measurement of selection on correlated characters. Evolution 37:1210–1226.

Lande, R., and S. H. Orzack. 1988. Extinction dynamics of age-structured populations in a fluctuating environment. Proceedings of the National Academy of Sciences of the USA 85:7418–7421.

Lynch, M., W. Gabriel, and A. M. Wood. 1991. Adaptive and demographic responses of plankton populations to environmental change. Limnology and Oceanography 36:1301–1312.

Lynch, M., and R. Lande. 1993. Evolution and extinction in response to environmental change. Pages 234–250 *in* P. Kareiva, J. G. Kingsolver, and R. B. Huey, eds. Biotic interactions and global change. Sinauer, Sunderland, MA.

Marshall, D. J., S. C. Burgess, and T. Connallon. 2016. Global change, life-history complexity and the potential for evolutionary rescue. Evolutionary Applications 9:1189– 1201.

McDonald, J. L., M. Franco, S. Townley, T. H. Ezard, K. Jelbert, and D. J. Hodgson. 2017. Divergent demographic strategies of plants in variable environments. Nature Ecology and Evolution 1:0029.

Morris, W. F., C. A. Pfister, S. Tuljapurkar, C. V. Haridas, C. L. Boggs, M. S. Boyce, E. M. Bruna, et al. 2008. Longevity can buffer plant and animal populations against changing climatic variability. Ecology 89:19–25.

Murphy, G. I. 1968. Pattern in life history and the environment. American Naturalist 102:391–403.

Orive, M. E., M. Barfield, C. Fernandez, and R. D. Holt. 2017. Effects of clonal reproduction on evolutionary lag and evolutionary rescue. American Naturalist 190:469–490.

Orzack, S. H., and S. Tuljapurkar. 1989. Population dynamics in variable environments. VII. The demography and evolution of iteroparity. American Naturalist 133:901–923.

Paniw, M., A. Ozgul, and R. Salguero-Gómez. 2018. Interactive life-history traits predict sensitivity of plants and animals to temporal autocorrelation. Ecology Letters 21:275–286.

Parmesan, C. 2006. Ecological and evolutionary responses to recent climate change. Annual Review of Ecology, Evolution, and Systematics 37:637–669.

Pearson, R. G., J. C. Stanton, K. T. Shoemaker, M. E. Aiello-Lammens, P. J. Ersts, N. Horning, D. A. Fordham, et al. 2014. Life history and spatial traits predict extinction risk due to climate change. Nature Climate Change 4:217–221.

Petit, R. J., and A. Hampe. 2006. Some evolutionary consequences of being a tree. Annual Review of Ecology, Evolution, and Systematics 37:187–214.

Polechová, J., N. Barton, and G. Marion. 2009. Species' range: adaptation in space and time. American Naturalist 174:E186–E204.

R Core Team. 2019. R: a language and environment for statistical computing. R Foundation for Statistical Computing, Vienna.

Sæther, B.-E., T. Coulson, V. Grøtan, S. Engen, R. Altwegg, K. B. Armitage, C. Barbraud, et al. 2013. How life history influences population dynamics in fluctuating environments. American Naturalist 182:743–759.

Salguero-Gómez, R. 2017. Applications of the fast-slow continuum and reproductive strategy framework of plant life histories. New Phytologist 213:1618–1624.

Salguero-Gómez, R., O. R. Jones, S. P. Blomberg, D. J. Hodgson, P. A. Zuidema, and H. D. Kroon. 2017. Fast-slow continuum and reproductive strategies structure plant life-history variation worldwide. Proceedings of the National Academy of Sciences of the USA 114:E9753.

Sasaki, A., and S. Ellner. 1997. Quantitative genetic variance maintained by fluctuating selection with overlapping generations: variance components and covariances. Evolution 51:682–696.

Schmid, M., M. Paniw, M. Postuma, A. Ozgul, and F. Guillaume. 2022. Data from: A trade-off between robustness to environmental fluctuations and speed of evolution. American Naturalist, Dryad Digital Repository, https://doi.org/10.5061/dryad.hx3ffbgdv.

Stearns, S. C. 1983. The influence of size and phylogeny on patterns of covariation among life-history traits in the mammals. Oikos 41:173–187.

———. 1989. Trade-offs in life-history evolution. Functional Ecology 3:259–268.

Stocker, T., D. Qin, G.-K. Plattner, M. Tignor, S. Allen, J. Boschung, A. Nauels, Y. Xia, V. Bex, and P. Midgley. 2013. IPCC, 2013: climate change 2013: the physical science basis. Contribution of Working Group I to the Fifth Assessment Report of the Intergovernmental Panel on Climate Change. Technical report, IPCC, Cambridge University Press, Cambridge.

Stubben, C. J., and B. G. Milligan. 2007. Estimating and analyzing demographic models using the popbio package in R. Journal of Statistical Software 22:11.

Svardal, H., C. Rueffler, and J. Hermisson. 2015. A general condition for adaptive genetic polymorphism in temporally and spatially

heterogeneous environments. Theoretical Population Biology 99:76–97.

Takada, T., and H. Nakajima. 1998. Theorems on the invasion process in stage-structured populations with density-dependent dynamics. Journal of Mathematical Biology 36:497–514.

Templeton, A. R., and D. A. Levin. 1979. Evolutionary consequences of seed pools. American Naturalist 114:232–249.

Tuljapurkar, S. 1982. Population dynamics in variable environments. III. Evolutionary dynamics of *r*-selection. Theoretical Population Biology 21:141–165.

———. 1990. Population dynamics in variable environments. Springer, Berlin.

Tuljapurkar, S., J. M. Gaillard, and T. Coulson. 2009. From stochastic environments to life histories and back. Philosophical Transactions of the Royal Society B 364:1499–1509.

Tuljapurkar, S., C. C. Horvitz, and J. B. Pascarella. 2003. The many growth rates and elasticities of populations in random environments. American Naturalist 162:489–502.

Ummenhofer, C. C., and G. A. Meehl. 2017. Extreme weather and climate events with ecological relevance: a review. Philosophical Transactions of the Royal Society B 372:20160135.

Van De Pol, M., Y. Vindenes, B.-E. Sæther, S. Engen, B. J. Ens, K. Oosterbeek, and J. M. Tinbergen. 2010. Effects of climate change and variability on population dynamics in a long-lived shorebird. Ecology 91:1192–1204.

Van Mantgem, P. J., and N. L. Stephenson. 2007. Apparent climatically induced increase of tree mortality rates in a temperate forest. Ecology Letters 10:909–916.

Vander Wal, E., D. Garant, M. Festa-Bianchet, and F. Pelletier. 2013. Evolutionary rescue in vertebrates: evidence, applications and uncertainty. Philosophical Transactions of the Royal Society B 368:20120090.

Vázquez, D. P., E. Gianoli, W. F. Morris, and F. Bozinovic. 2015. Ecological and evolutionary impacts of changing climatic variability. Biological Reviews 92:22–42.

Wolfram Research. 2020. Mathematica.

Yamamichi, M., N. G. Hairston Jr., M. Rees, and S. P. Ellner. 2019. Rapid evolution with generation overlap: the double-edged effect of dormancy. Theoretical Ecology 12:179–195.

Zeineddine, M., and V. A. A. Jansen. 2009. To age, to die: parity, evolutionary tracking and Cole's paradox. Evolution 63:1498–1507.

Associate Editor: David Vasseur
Editor: Jennifer A. Lau

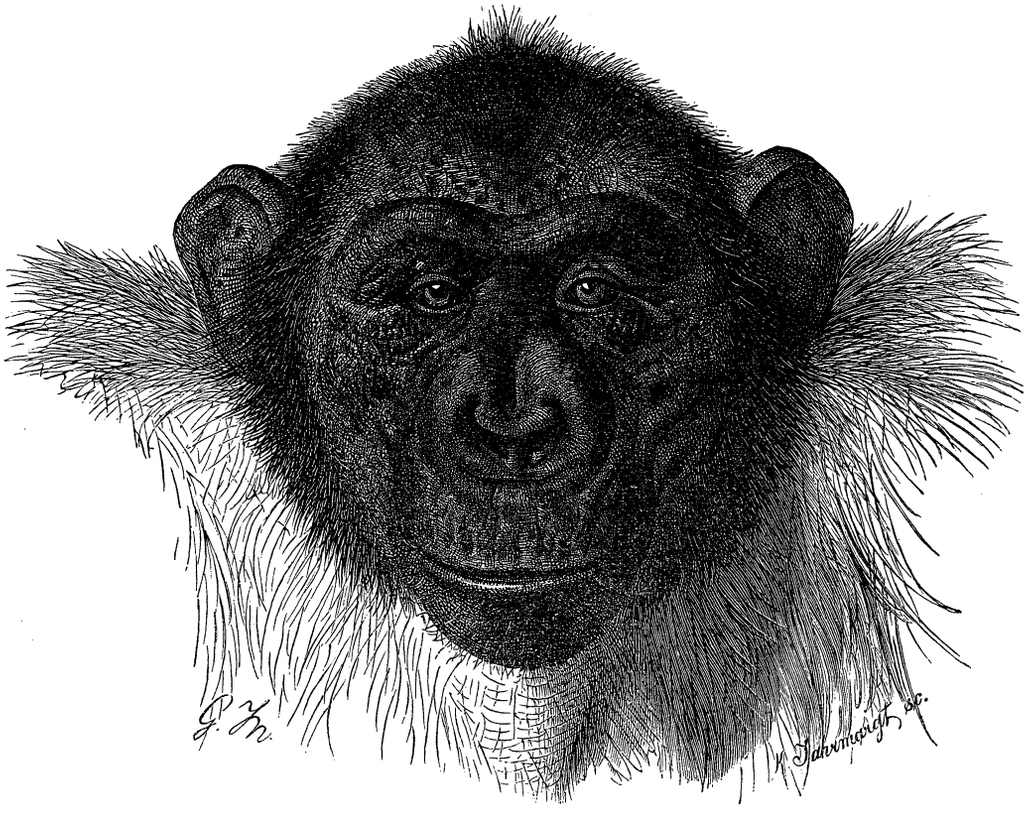

"Then succeeds a more special account of the gorilla, the chimpanzee, and the tschego (*Anthropopithecus tschego*) [figured], and orang." From the review of Brehm's *Animal Life* (*The American Naturalist*, 1877, 11:557–559).